Wave Patterns for Solutions to Semilinear Equations

$$u_{tt} = u_{xx} + f(u)$$

Michael Taylor

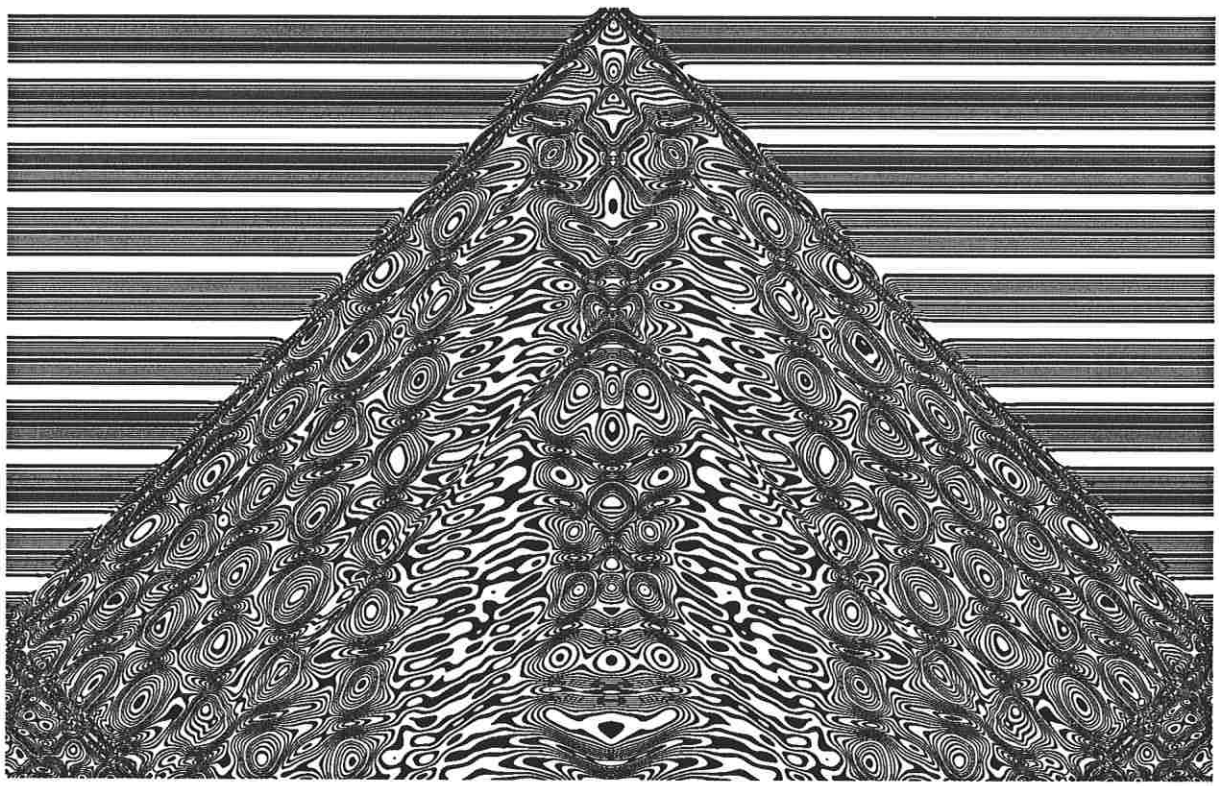

CONTENTS

1. Introduction
2. Difference schemes: first versions
3. Wave graphs
4. Symmetry
5. Wave patterns

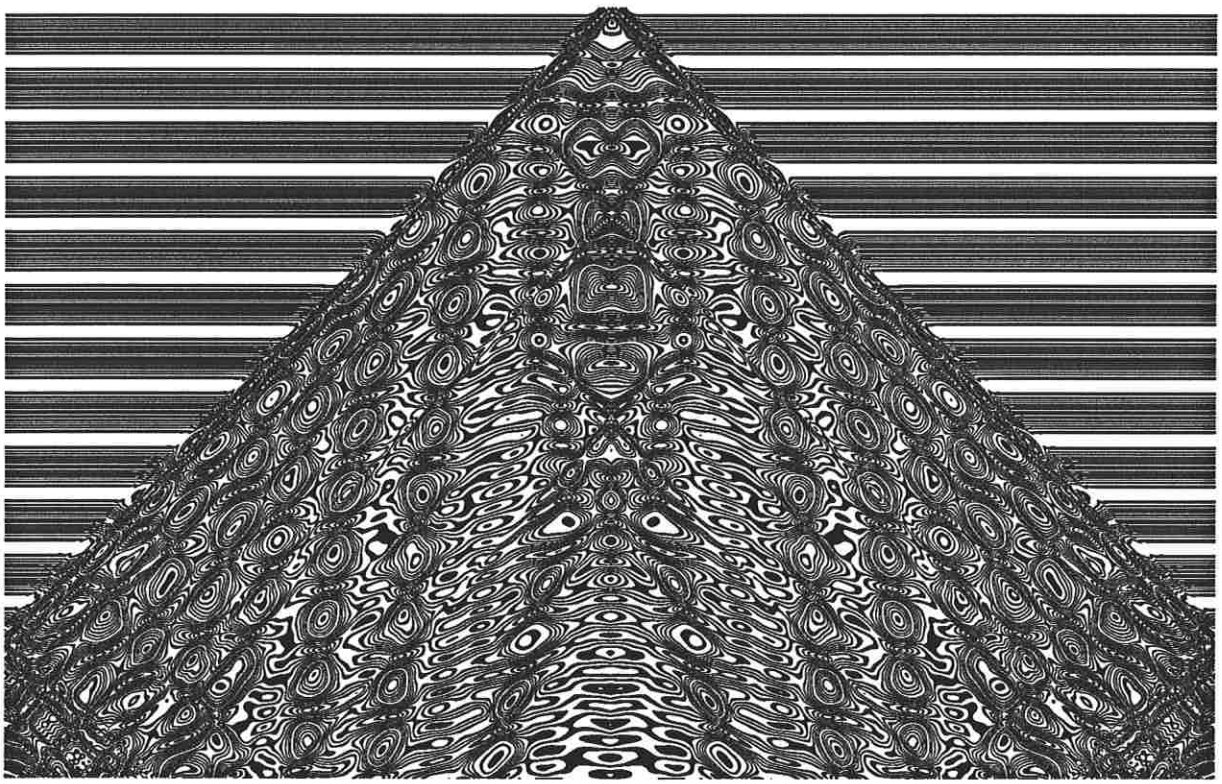

1. Introduction

Our goal is to present a graphical study of solutions to semilinear wave equations of the form

$$u_{tt} = u_{xx} + f(u). \tag{1.1}$$

We were motivated to do this in order to look into remarks on these equations made in [W], pp. 161–166. Realizing from experience that Mathematica's PDE solver is built for comfort, not for speed, we decided to write our own programs. There are several well known second-order accurate schemes that apply to (1.1), including a straightforward centered difference scheme and Lax-Wendroff schemes. Rather than going with them, we decided it would be simple enough to take advantage of the special structure of (1.1) to produce higher-order accurate schemes.

In §2 we produce a third-order accurate difference scheme for (1.1) (and, as an intermediate step, a second-order accurate scheme), derived from a pair of integral equations in a fashion somewhat parallel to the production of Runge-Kutta schemes for ODE. In §3 we present graphs of solutions, with various functions $f(u)$, obtained by running these schemes. Examples range from the tamely behaved Sine-Gordon equation to the more chaotic sort mentioned in [W]. In the wilder cases, deviation of the approximations graphed here from the true solution is manifested in two ways: in how the results of the second and third-order accurate schemes differ, and in how the bilateral symmetry present in the initial condition eventually deteriorates. In §4 we produce more complex difference schemes that enforce this symmetry and present more graphs. We also compare the performance of the standard centered difference scheme.

In §5 we get to the good stuff, the presentation of wave patterns for solutions to (1.1), with various functions $f(u)$. These wave patterns are obtained essentially as contour plots of the solutions. Some cases show intriguing complexity, while others yield simpler patterns. At this stage, these patterns are presented basically as food for thought, though no doubt there are theorems to be proven about the degree of complexity and chaos manifested in some of these semilinear wave equations.

WARNING. Gazing at some of these wave patterns can be addicting.

2. Difference schemes: first versions

Our schemes will be produced by techniques reminiscent of those used to produce the Runge-Kutta scheme for ODE. They will make strong use of the special structure of (1.1). To begin, we set $v = u_t + u_x$ and rewrite (1.1) as a first-order system:

$$\begin{aligned} u_t + u_x &= v, \\ v_t - v_x &= f(u). \end{aligned} \tag{2.1}$$

To work on this, consider $\xi(s) = u(t+s, x+s)$ and $\zeta(s) = v(t+s, x-s)$, which satisfy

$$\xi'(s) = v(t+s, x+s), \quad \zeta'(s) = f\big(u(t+s, x-s)\big). \tag{2.2}$$

Hence a solution to (2.1) satisfies

$$\begin{aligned} u(t,x) &= u(t-h, x-h) + \int_0^h v(t-h+s, x-h+s)\, ds, \\ v(t,x) &= v(t-h, x+h) + \int_0^t f\big(u(t-h+s, x+h-s)\big)\, ds. \end{aligned} \tag{2.3}$$

To discretize these identities, keep in mind the following formulas regarding use of the trapedoidal rule and Simpson's rule:

$$\int_0^h \varphi(s)\, ds = \frac{h}{2}\big[\varphi(0) + \varphi(h)\big] + O(h^3), \tag{2.4}$$

$$\int_0^h \varphi(s)\, ds = \frac{h}{6}\Big[\varphi(0) + 4\varphi\Big(\frac{h}{2}\Big) + \varphi(h)\Big] + O(h^5), \tag{2.5}$$

valid for sufficiently smooth φ. Note that if we can approximate all the terms $\varphi(\sigma)$ on the right side of (2.4) within $O(h^2)$, then we have the left side to $O(h^3)$. If we can approximate all terms $\varphi(\sigma)$ in the right side of (2.5) within $O(h^3)$, we have the left side to $O(h^4)$.

We are prepared to produce difference schemes for approximations u_{jk} and v_{jk} to $u(jh, kh)$ and $v(jh, kh)$, respectively, where h (the step size) is a given small quantity. Making use of (2.3) and (2.4), we have the following second-order accurate difference scheme:

$$\begin{aligned} v_{jk} &= v_{j-1,k+1} + \frac{h}{2}\big[f(u_{j-1,k+1}) + f(u_{j-1,k-1} + hv_{j-1,k-1})\big], \\ u_{jk} &= u_{j-1,k-1} + \frac{h}{2}\big[v_{j-1,k-1} + v_{jk}\big]. \end{aligned} \tag{2.6}$$

Bringing in (2.5), we see that a third-order accurate scheme can be produced in the form

$$
\begin{aligned}
u_{jk} &= u_{j-1,k-1} + \frac{h}{6}\big[v_{j-1,k-1} + 4\hat{v}_{j-1/2,k-1/2} + \hat{v}_{jk}\big], \\
v_{jk} &= v_{j-1,k+1} + \frac{h}{6}\big[f(u_{j-1,k+1}) + 4f(\hat{u}_{j-1/2,k+1/2}) + f(u_{jk})\big],
\end{aligned} \tag{2.7}
$$

provided $\hat{v}_{j-1/2,k-1/2}$ and $\hat{v}_{jk}$ are given by second-order accurate difference schemes, e.g.,

$$
\begin{aligned}
\hat{v}_{j-1/2,k-1/2} &= v_{j-1,k} + \frac{h}{4}\Big[f(u_{j-1,k}) + f\Big(u_{j-1,k-1} + \frac{h}{2}v_{j-1,k-1}\Big)\Big], \\
\hat{v}_{jk} &= v_{j-1,k+1} + \frac{h}{2}\big[f(u_{j-1,k+1}) + f(u_{j-1,k-1} + hv_{j-1,k-1})\big],
\end{aligned} \tag{2.8}
$$

as suggested by (2.6), and provided also that $\hat{u}_{j-1/2,k+1/2}$ is given by a second-order accurate scheme, e.g.,

$$
\hat{u}_{j-1/2,k+1/2} = u_{j-1,k} + \frac{h}{4}\Big[v_{j-1,k} + v_{j-1,k+1} + \frac{h}{2}f(u_{j-1,k+1})\Big]. \tag{2.9}
$$

It is clear that the scheme defined by (2.7)–(2.9) satisfies the Lewy condition. See Figure A for a picture of what data are used to compute u_{jk} and v_{jk}. Results of running the scheme verify its stability.

In principle we could turn the crank once more and produce a fourth-order accurate scheme. (Compare the analysis in §3 of [T].) However, we have not put forth the effort to do this here.

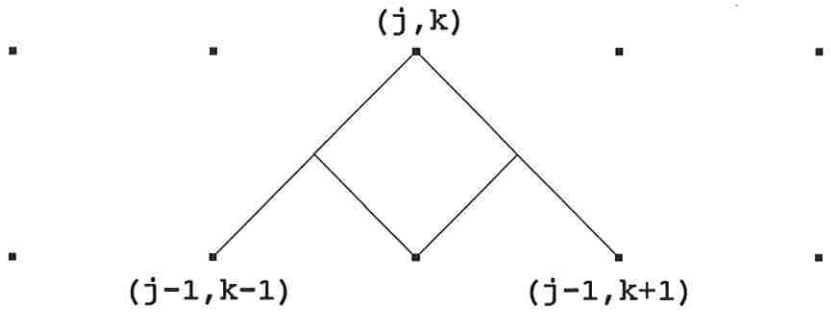

Figure A

3. Wave graphs

Here we present graphs of solutions to

$$u_{tt} = u_{xx} + f(u) \tag{3.1}$$

for a variety of functions $f(u)$, namely

$$f(u) = (1 - u^2)(1 + 4u), \tag{3.2}$$

$$f(u) = -\sin u, \tag{3.3}$$

$$f(u) = -u - u^3, \tag{3.4}$$

$$f(u) = u - u^3. \tag{3.5}$$

The case (3.2) is treated in Figures 1–1Y, the case (3.3) in Figures 2–2Z, the case (3.4) in Figures 3–3C, and the case (3.5) in Figures 4–4Z. In some of these figures it is noted that a second-order accurate scheme (i.e., (2.6)) is used. If not otherwise noted, we use the third-order accurate scheme (2.7)–(2.9). In all cases we take $h = 0.02$, and initial data

$$u(0, x) = 2.3\, e^{-8x^2}, \quad u_t(0, x) = 0, \tag{3.6}$$

periodized, so $u(t, x)$ is periodic in x of period $639/50$. More precisely, $u(t, x)$ is approximated by $u(jh, (k - 320)h) = u_{jk}$, and u_{jk} is periodic in k of period 639. The value of N written below each graph is the number of iterations used, so the elapsed time from the initial condition (3.6) is equal to $T(N) = N/50$.

The case (3.2) is mentioned in [W], p. 165, as one leading to complex behavior along the lines of a class 4 cellular automaton. The case (3.3) gives the familiar Sine-Gordon equation, whose behavior is expected to be rather tame. The case (3.4) is a variant of the cubic Klein-Gordon equation, also tamely behaved. The case (3.5) differs from (3.4) in the sign on u. This allows for a growing mode of small-amplitude waves, and creates waves more complex than arising from (3.3) or (3.4), though not as complex as those arising from (3.2).

One aspect of these graphs worth pondering involves bilateral symmetry. Given the initial data (3.6), we see that the solution to (3.1) must be invariant under $x \mapsto -x$ for each t. In the case (3.2) we see in Figures 1–1B that this symmetry holds for u_{jk} (with respect to $k \mapsto 320 - k$) up through $j = N = 1500$, but it breaks down for $N = 2000$. For the second-order scheme applied to this equation, pictured in Figures 1X–1Y, one sees that bilateral symmetry is slightly off at $N = 1500$ and completely off at $N = 2000$.

The breaking of the symmetry $x \mapsto -x$ arises from the use of (2.1). In §4 we discuss how to replace (2.1) by a 3×3 system and discretize it in a fashion that produces difference schemes that do not break this symmetry.

As a perusal of Figures 2–2Z shows, the bilateral symmetry is not broken for the Sine-Gordon equation (case (3.3)) at any stage $N \leq 10000$, either for the third-order accurate

scheme (2.7)–(2.9) or even for the second-order accurate scheme (2.6). The same goes for case (3.4), as shown in Figures 3–3C, at least as far as the third-order accurate scheme is concerned.

Figures 4–4C, presenting results of the third-order accurate scheme in case (3.5), show a preservation of bilateral symmetry through $N = 4000$, a slight breakdown at $N = 6000$, and a complete breakdown at $N = 8000$. Figures 4Y–4Z show graphs produced via the second-order accurate scheme. The graphs in Figure 4Y agree with those in Figure 4B up through $N = 1000$, and differ only slightly at $N = 1500$. There is a greater difference at $N = 2000$, with a slight breakdown in symmetry in Figure 4Y, and a still greater difference at $N = 2500$, with a more substantial break in symmetry in Figure 4Y. Figure 4Z shows even more substantial breakdown at $N = 4000$.

The breaking of the bilateral symmetry certainly has undesirable aspects, and this motivates our work in the next section. However, it also has a valuable aspect, as an internal check on the accuracy of the approximate solutions derived via our difference schemes. Of course, it is more reliable as a negative indicator than as a positive indicator.

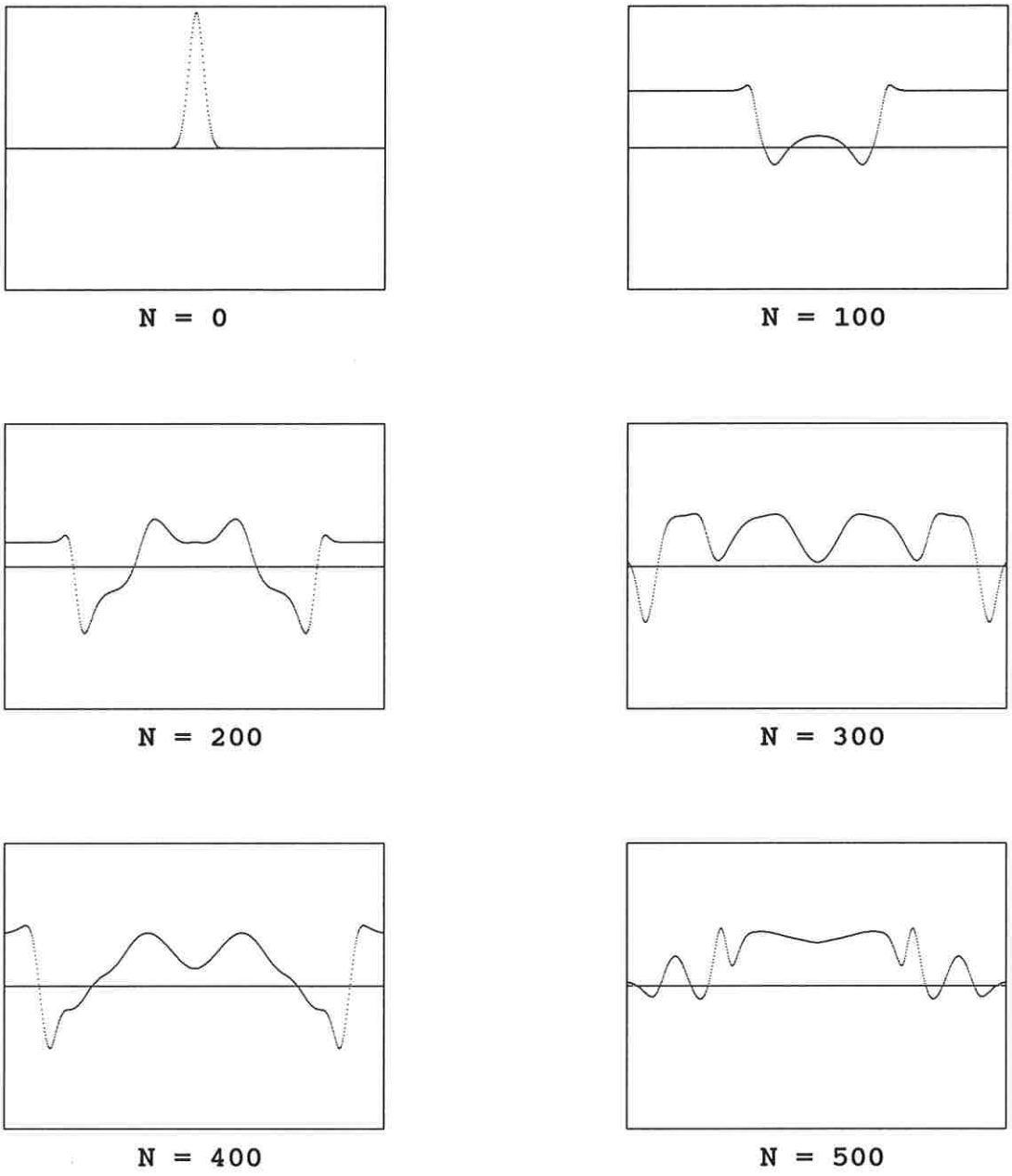

Figure 1

Solution to $u_{tt} = u_{xx} + (1 - u^2)(1 + 4u)$

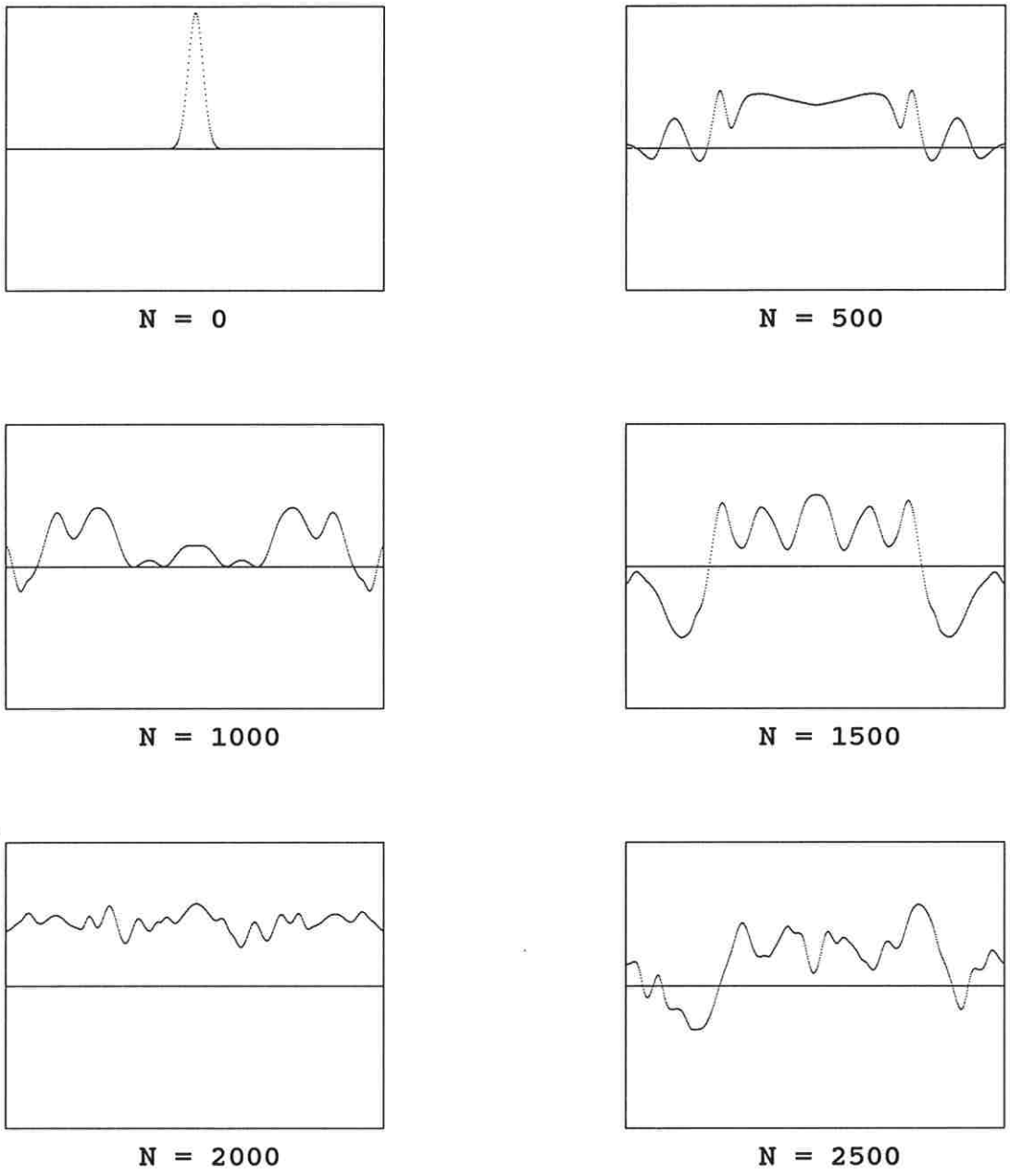

Figure 1B

Solution to $u_{tt} = u_{xx} + (1 - u^2)(1 + 4u)$

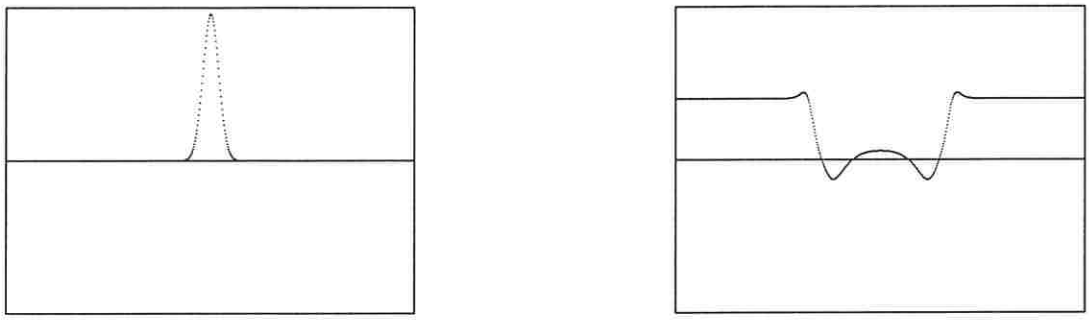

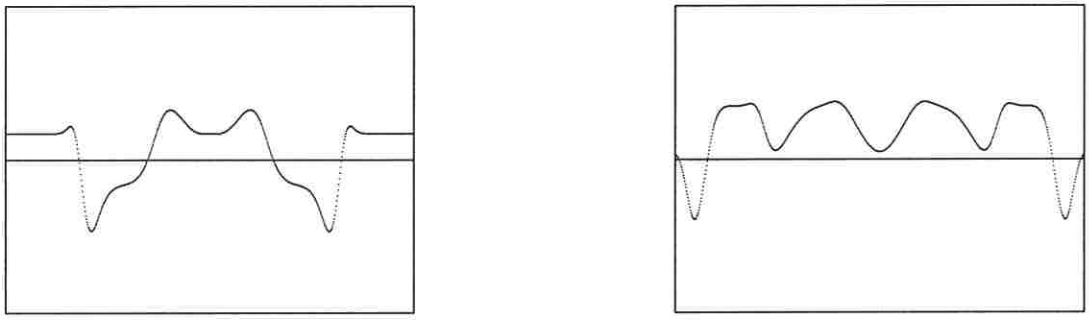

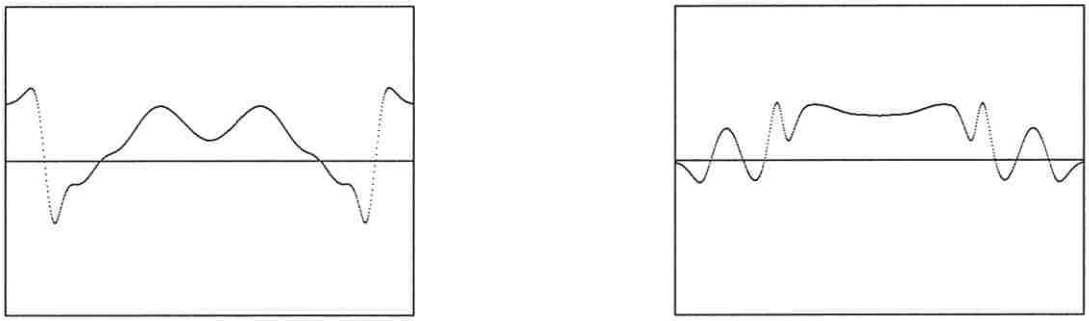

Figure 1X

Solution to $u_{tt} = u_{xx} + (1 - u^2)(1 + 4u)$

Second Order Accurate Scheme

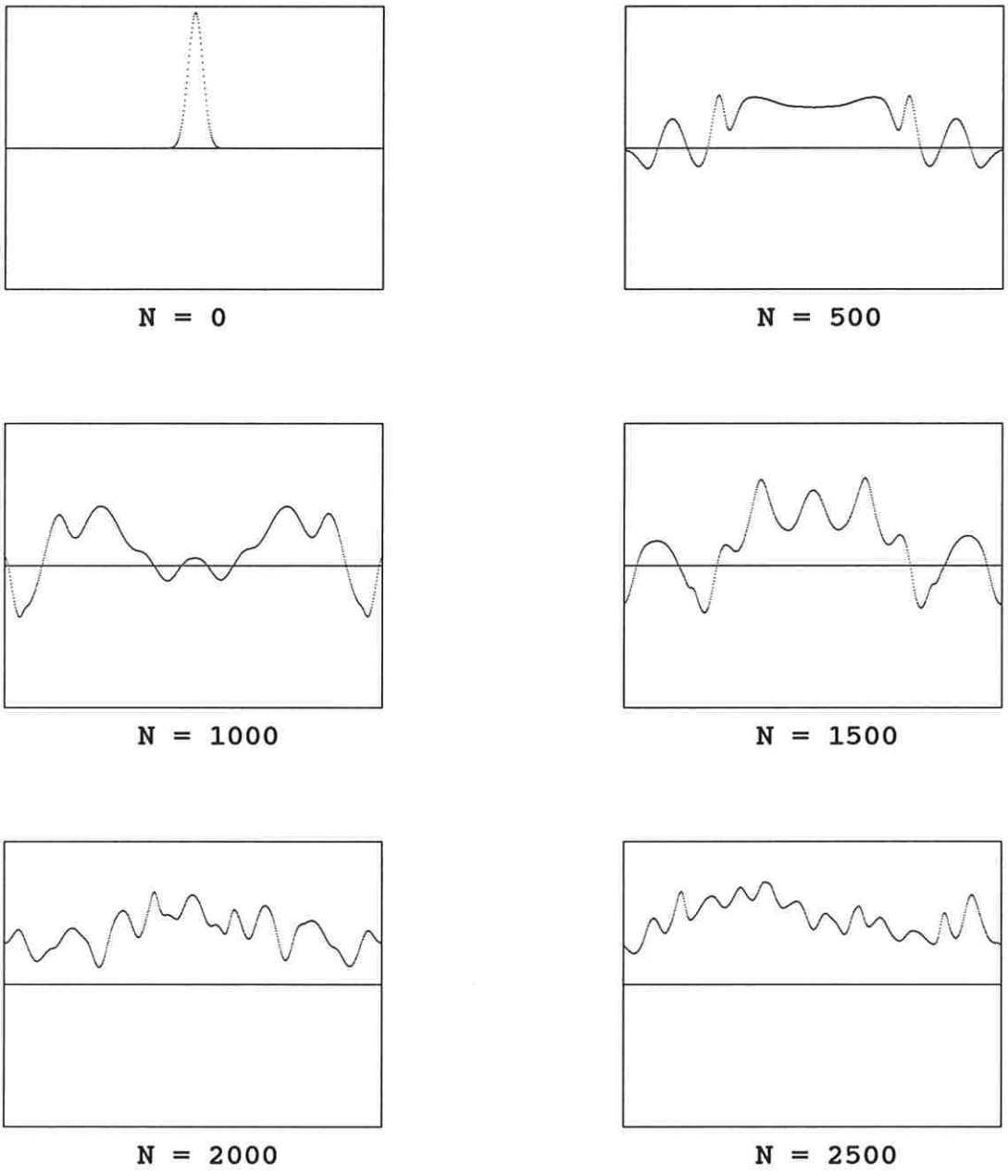

Figure 1Y

Solution to $u_{tt} = u_{xx} + (1 - u^2)(1 + 4u)$

Second Order Accurate Scheme

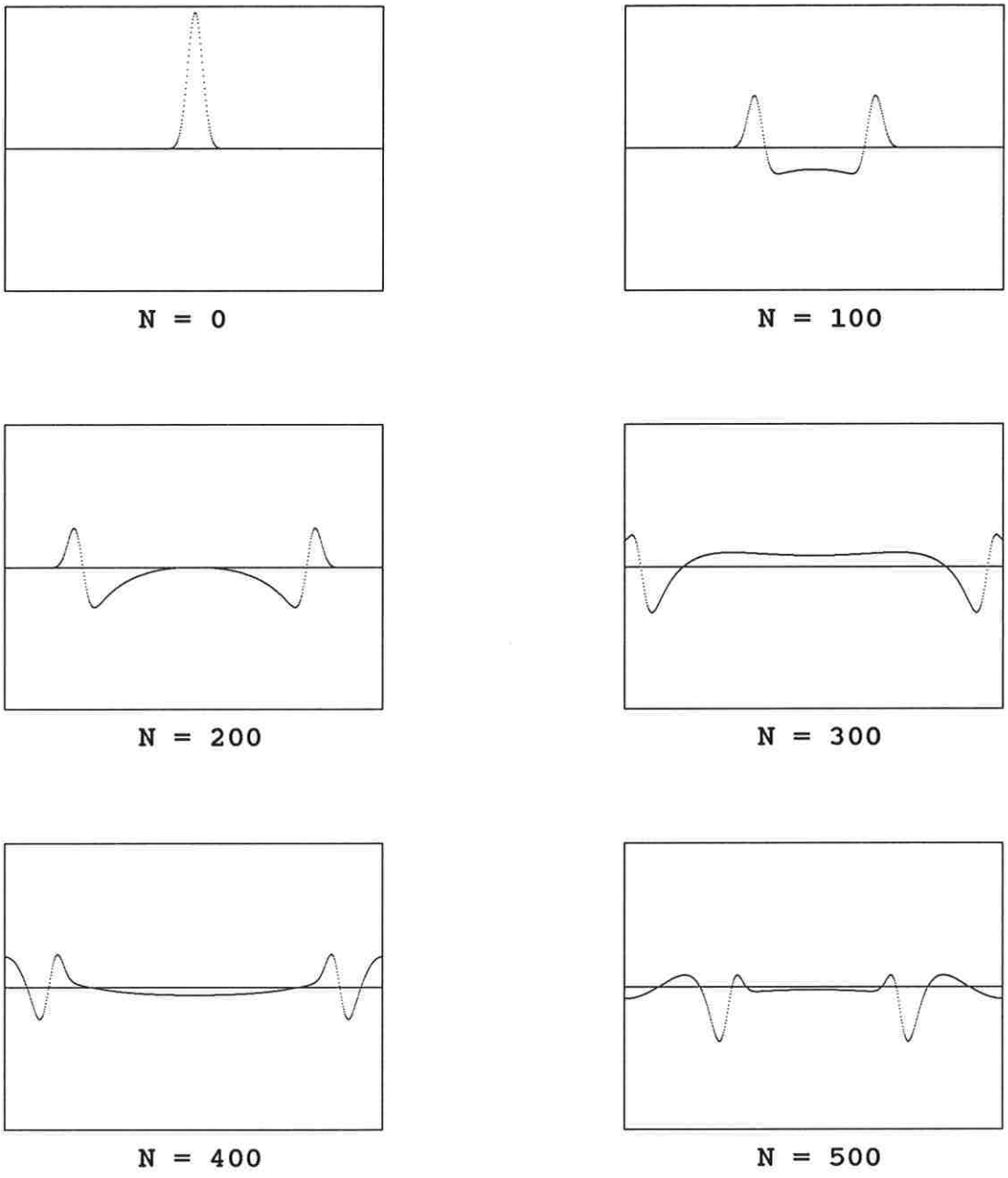

Figure 2

Solution to $u_{tt} = u_{xx} - \sin u$

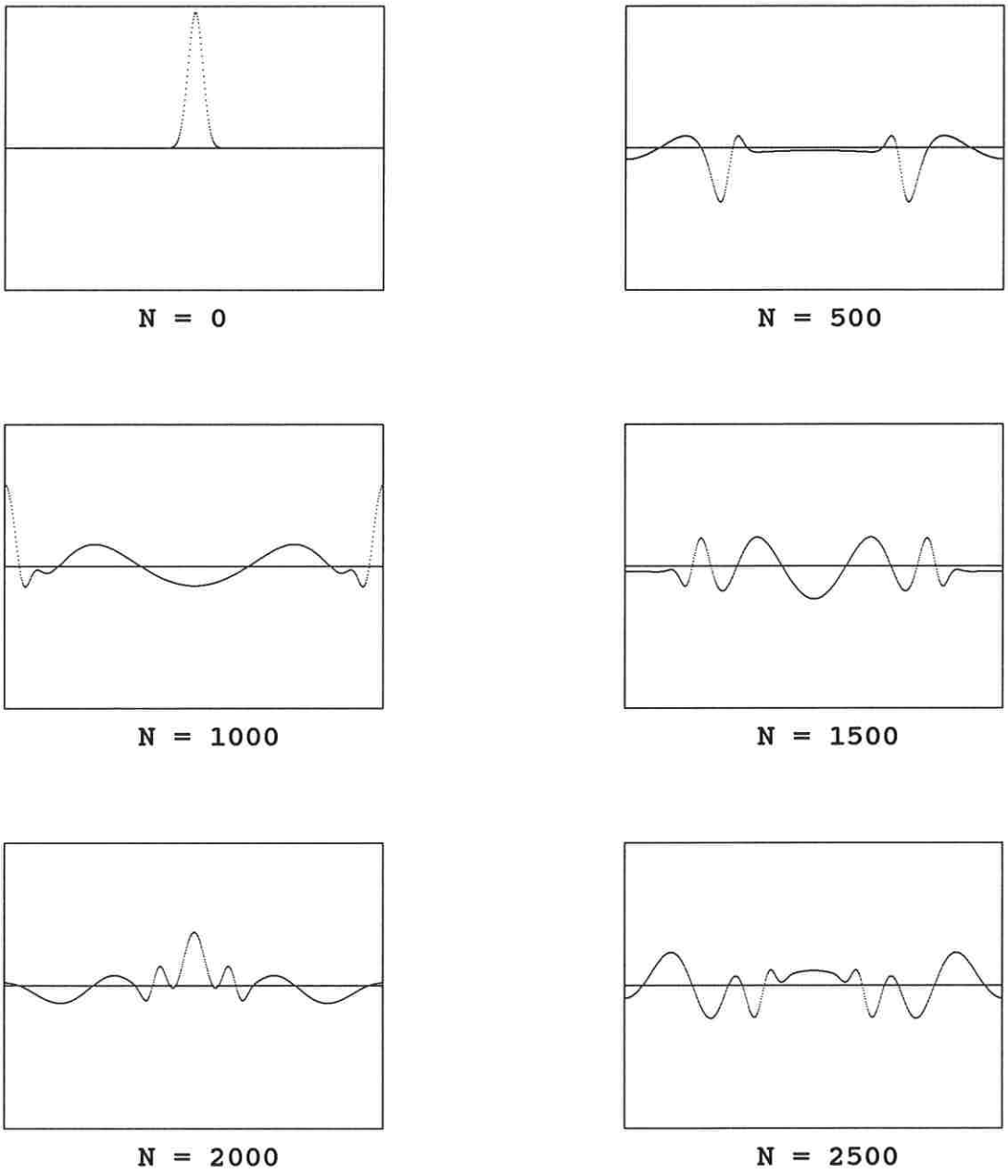

Figure 2B

Solution to $u_{tt} = u_{xx} - \sin u$

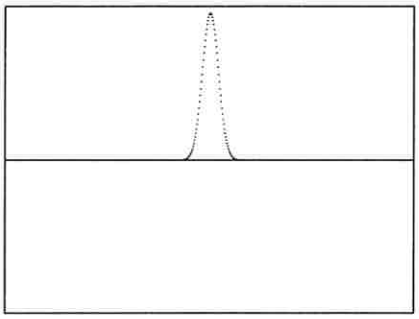

N = 0

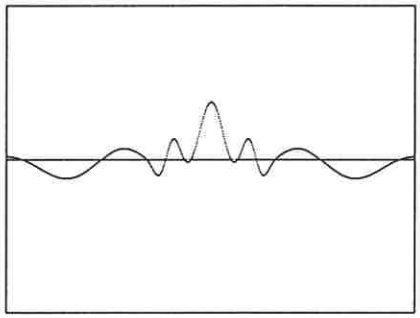

N = 2000

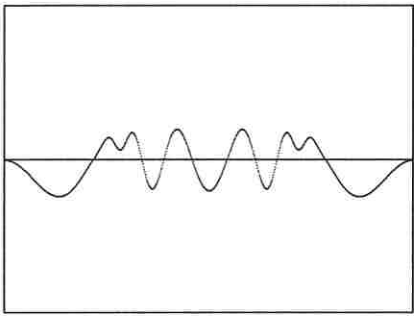

N = 4000

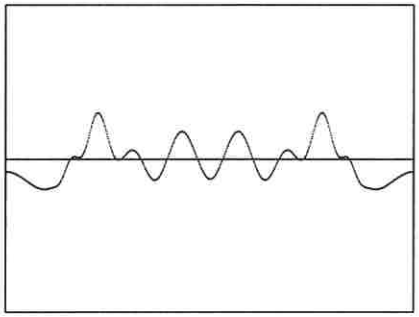

N = 6000

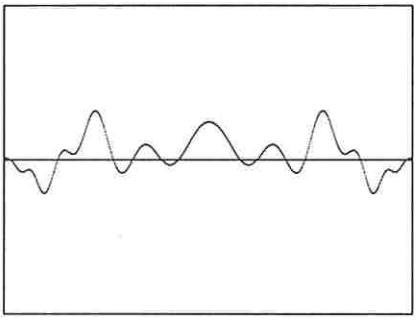

N = 8000

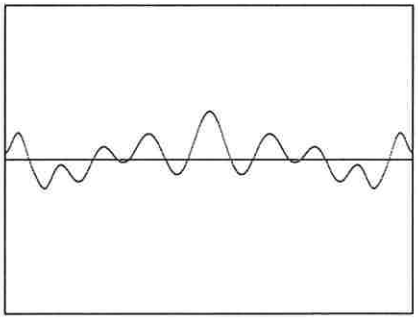

N = 10000

Figure 2C

Solution to $u_{tt} = u_{xx} - \sin u$

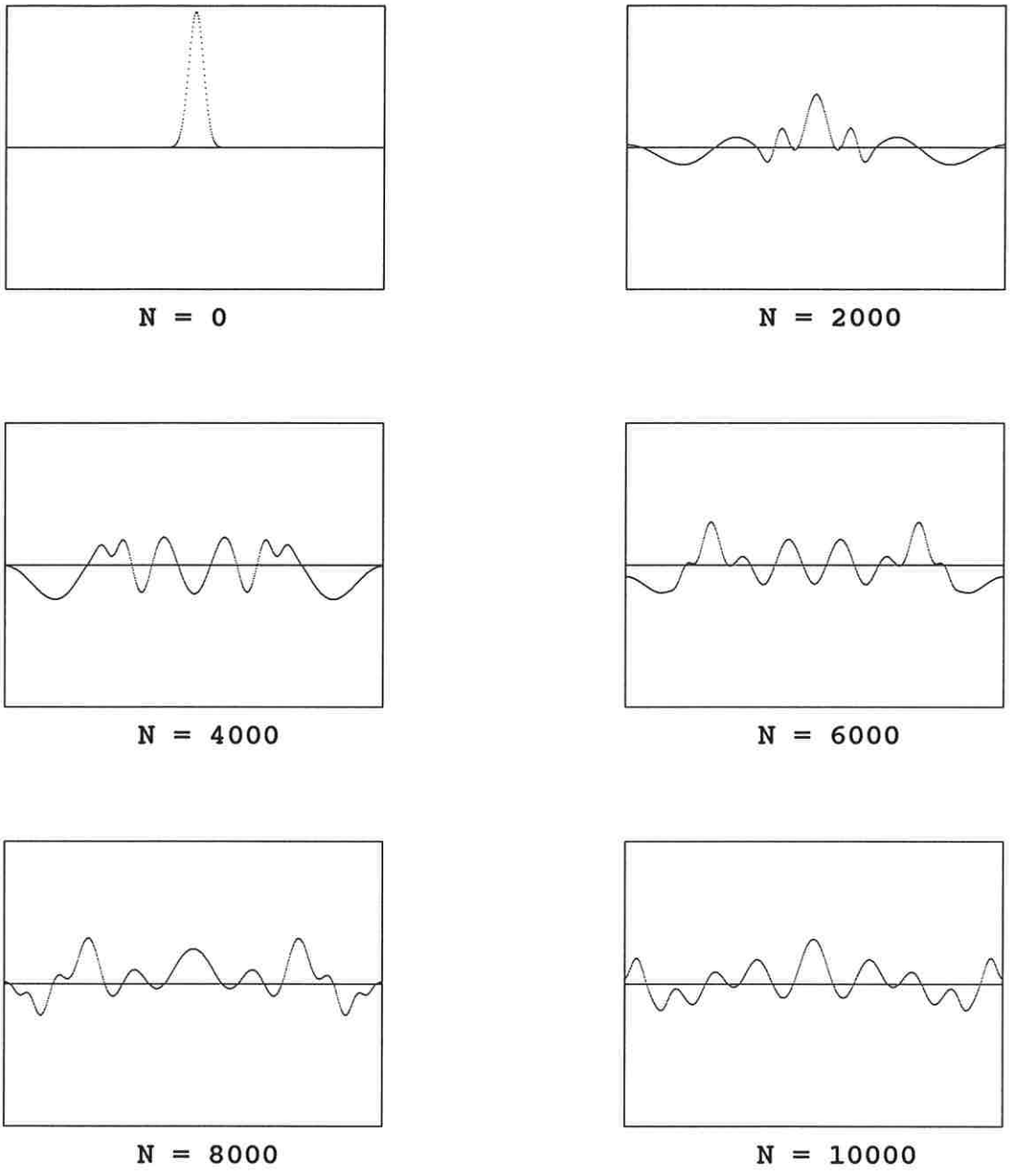

Figure 2Z

Solution to $u_{tt} = u_{xx} - \sin u$

Second Order Accurate Scheme

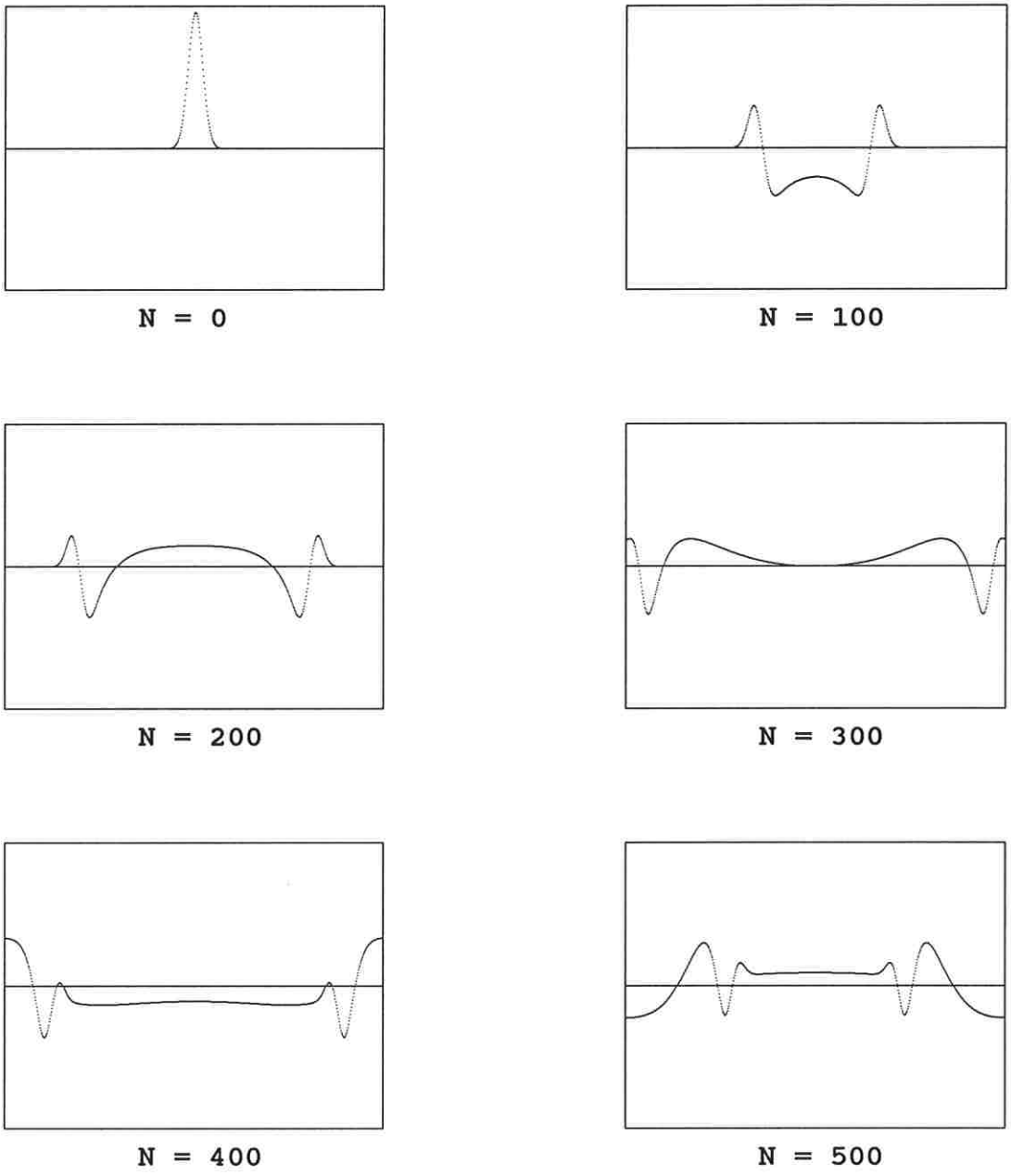

Figure 3

Solution to $u_{tt} = u_{xx} - u - u^3$

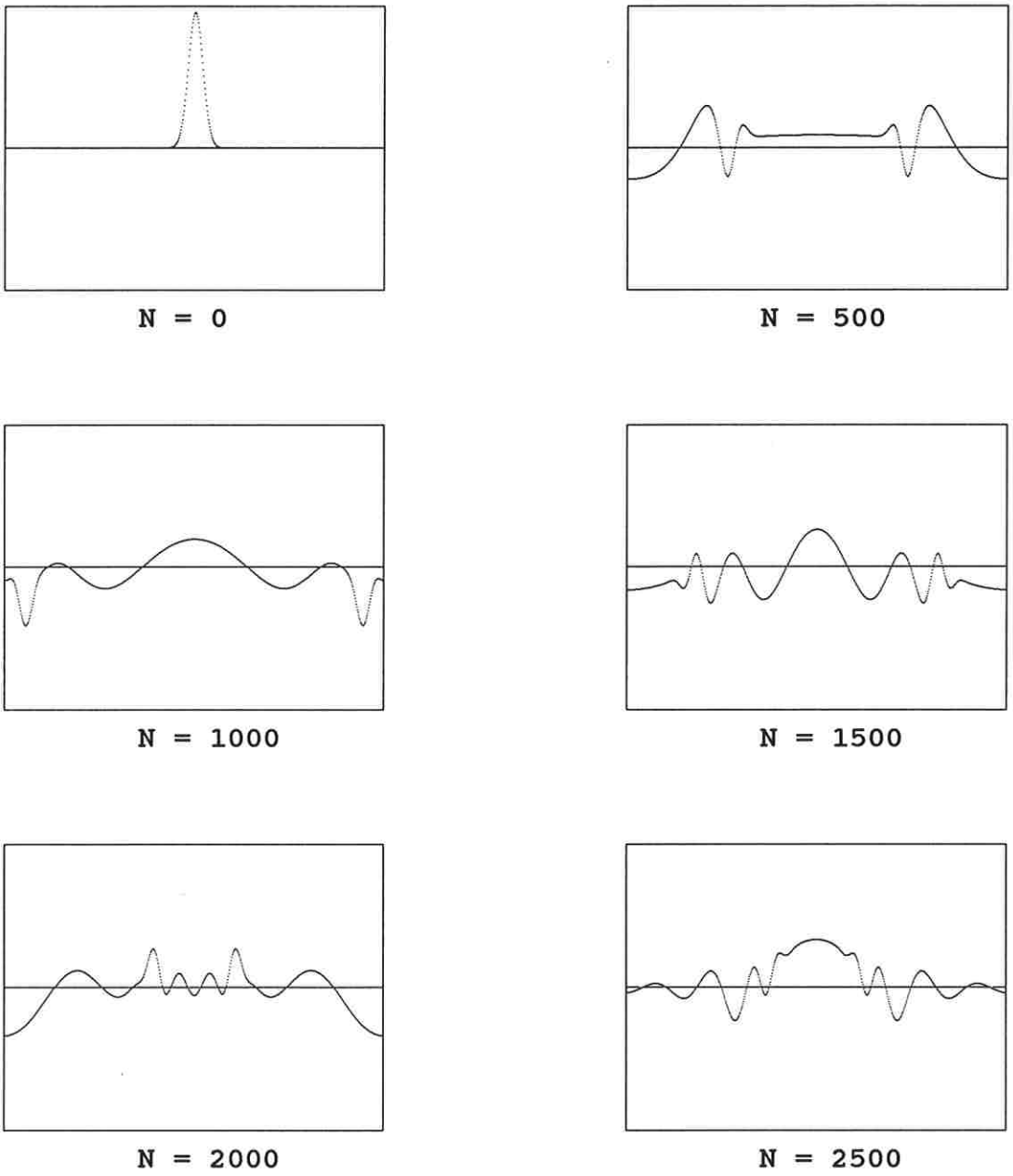

Figure 3B

Solution to $u_{tt} = u_{xx} - u - u^3$

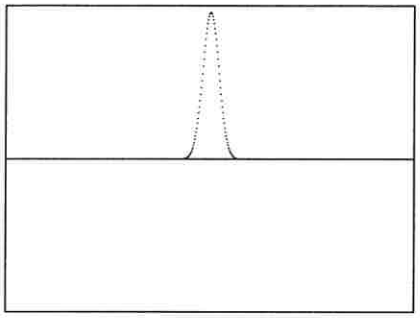

N = 0

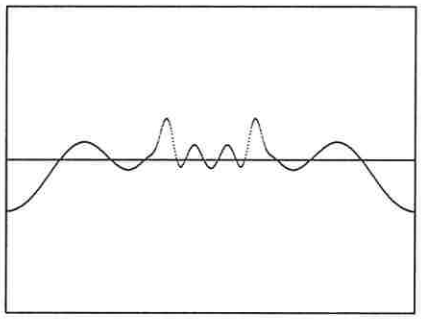

N = 2000

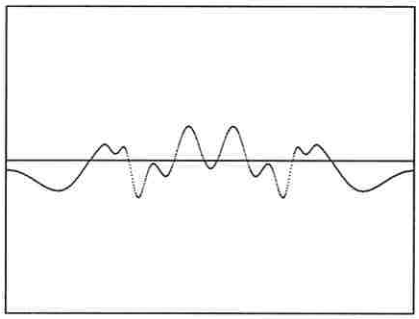

N = 4000

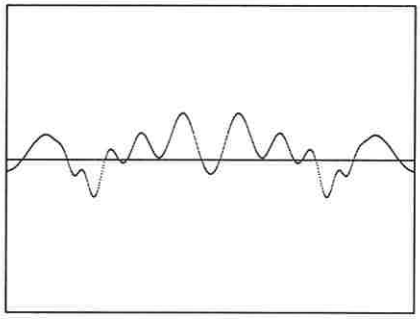

N = 6000

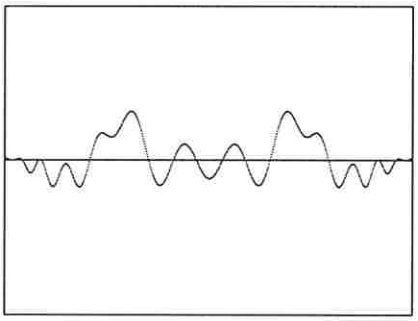

N = 8000

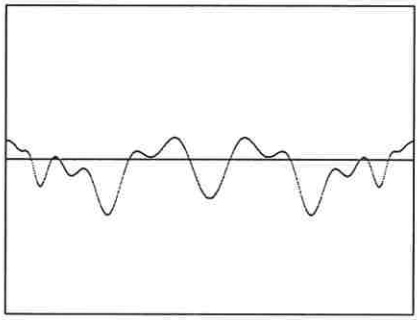

N = 10000

Figure 3C

Solution to $u_{tt} = u_{xx} - u - u^3$

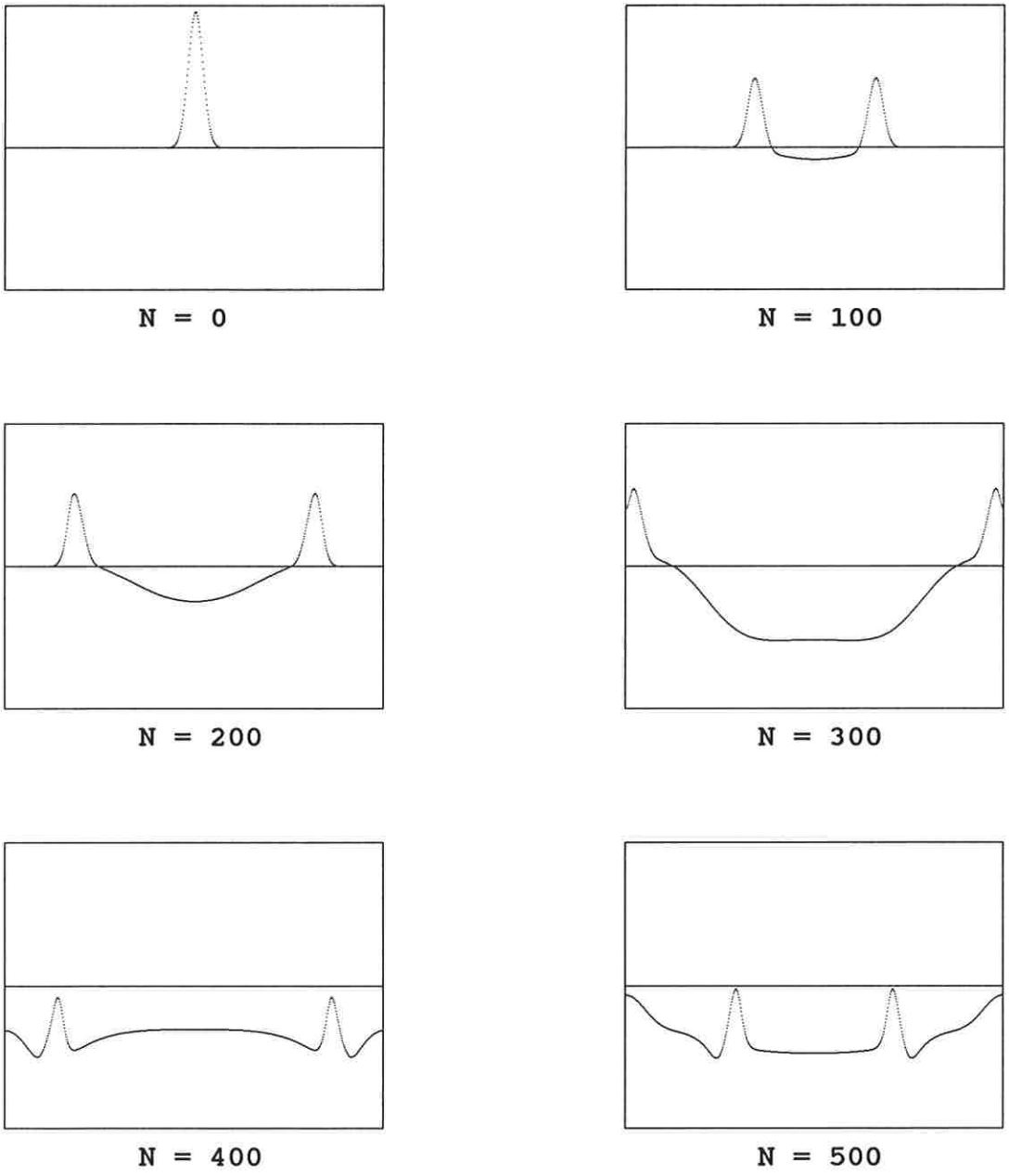

Figure 4

Solution to $u_{tt} = u_{xx} + u - u^3$

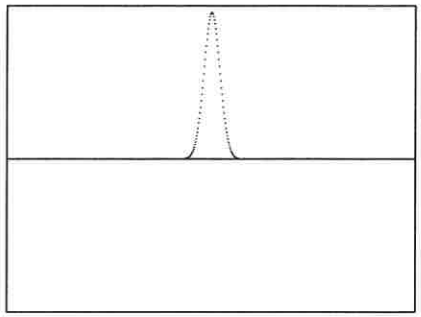

N = 0

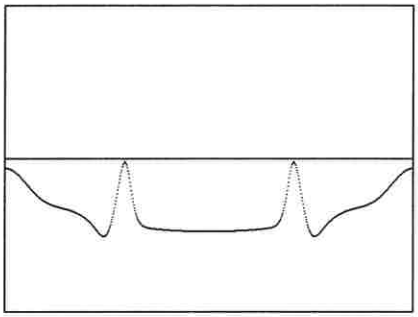

N = 500

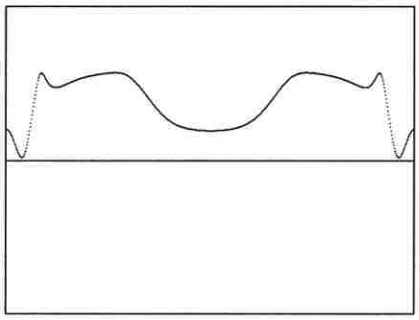

N = 1000

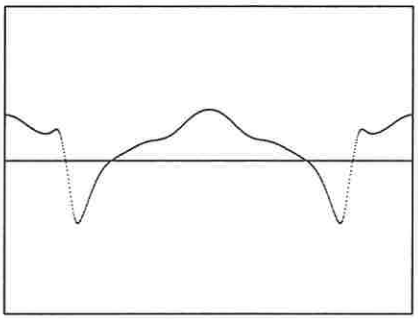

N = 1500

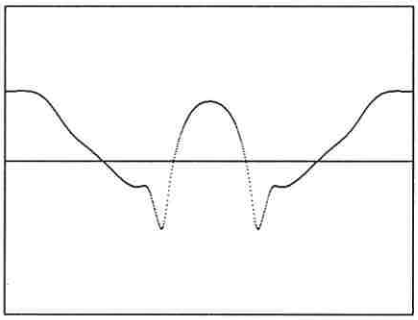

N = 2000

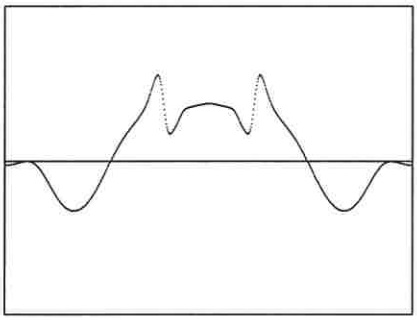

N = 2500

Figure 4B

Solution to $u_{tt} = u_{xx} + u - u^3$

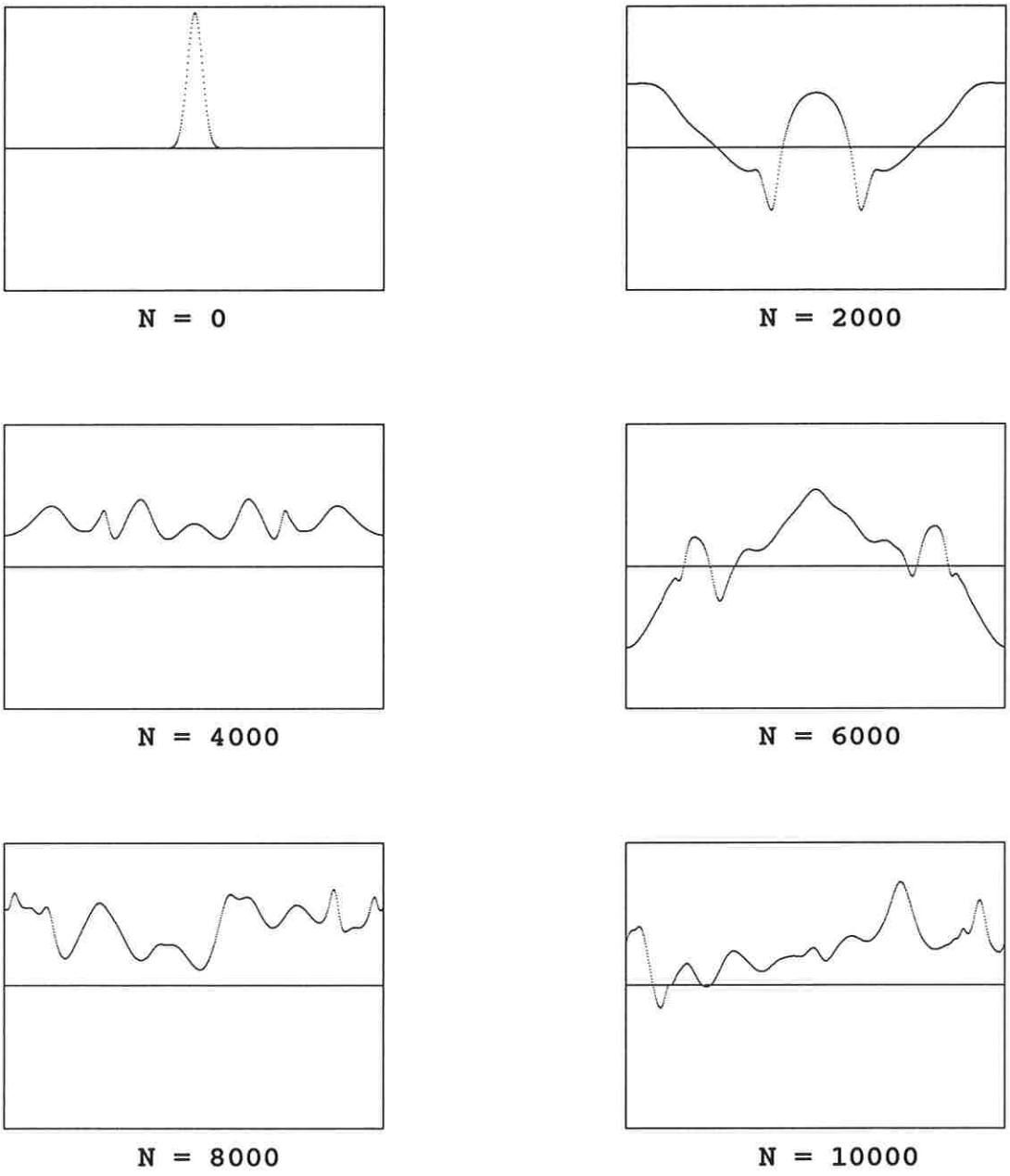

Figure 4C

Solution to $u_{tt} = u_{xx} + u - u^3$

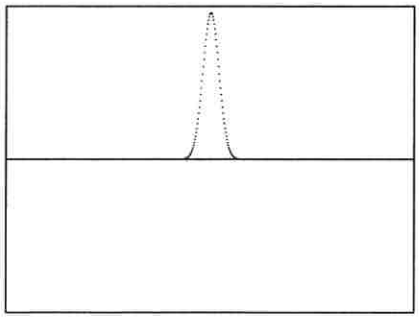

N = 0

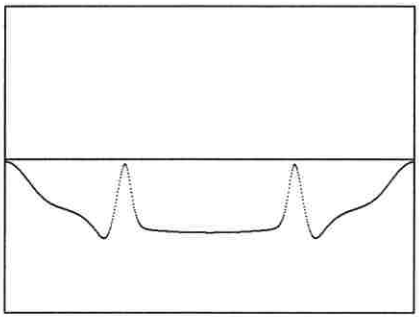

N = 500

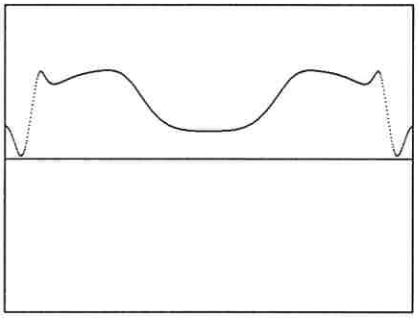

N = 1000

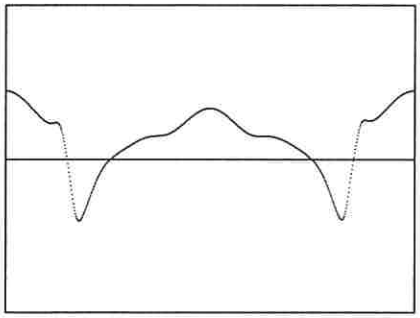

N = 1500

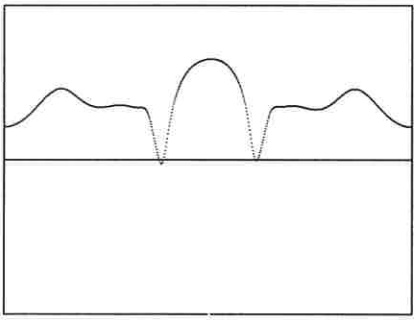

N = 2000

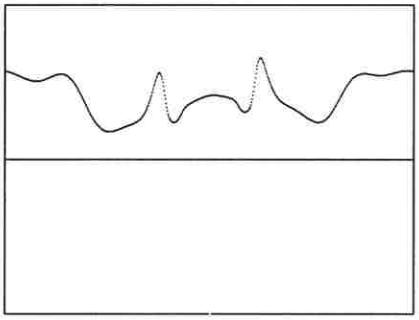

N = 2500

Figure 4Y

Solution to $u_{tt} = u_{xx} + u - u^3$

Second Order Accurate Scheme

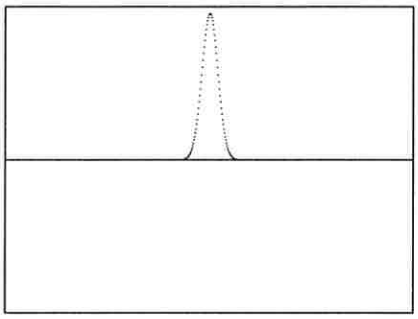

N = 0

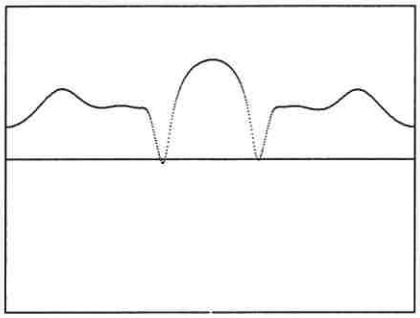

N = 2000

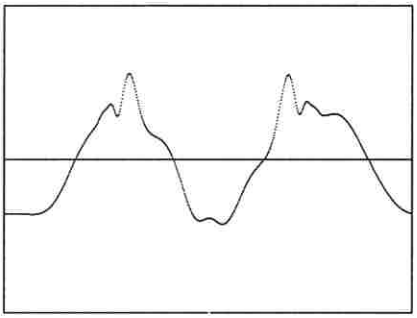

N = 4000

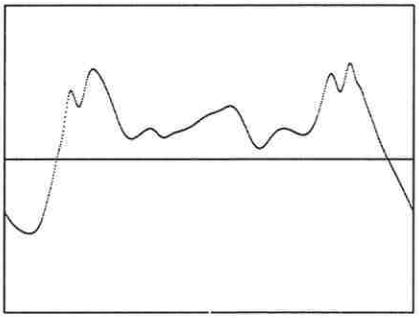

N = 6000

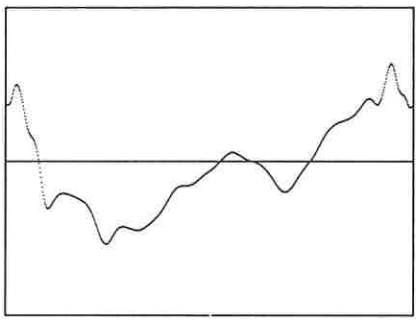

N = 8000

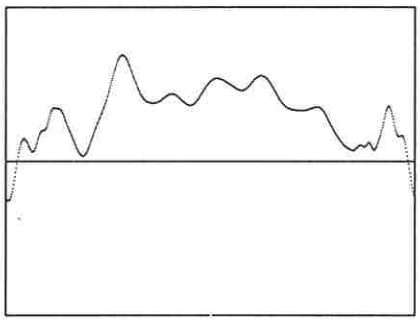

N = 10000

Figure 4Z

Solution to $u_{tt} = u_{xx} + u - u^3$

Second Order Accurate Scheme

4. Symmetry

As we have noted, despite the fact that (1.1) is invariant under the flip maps

$$x \mapsto c - x, \tag{4.1}$$

the difference schemes (2.6) and (2.7)–(2.9) break this symmetry. The culprit is (2.1), which lacks this symmetry. To restore it, we can bring in $w = u_t - u_x$, and replace (2.1) by the 3×3 system

$$\begin{aligned} v_t - v_x &= f(u), \\ w_t + w_x &= f(u), \\ u_t &= \frac{1}{2}(v + w). \end{aligned} \tag{4.2}$$

The following is a second order accurate scheme that respects the symmetry (4.1). We begin with

$$\begin{aligned} v_{jk} &= v_{j-1,k+1} + \frac{h}{2}\big[f(u_{j-1,k+1}) + f(\hat{u}_{jk})\big], \\ w_{jk} &= w_{j-1,k-1} + \frac{h}{2}\big[f(u_{j-1,k-1}) + f(\hat{u}_{jk})\big], \end{aligned} \tag{4.3}$$

where

$$\hat{u}_{jk} = u_{j-1,k} + \frac{h}{2}(v_{j-1,k} + w_{j-1,k}), \tag{4.4}$$

and then we take

$$u_{jk} = u_{j-1,k} + \frac{h}{4}(v_{jk} + w_{jk} + v_{j-1,k} + w_{j-1,k}). \tag{4.5}$$

Results of running this when $f(u) = (1 - u^2)(1 + 4u)$ are presented in Figures 5 and 5B. The graphs in Figure 5 are virtually indistinguishable from those of Figure 1X. The slight difference in case $N = 500$ moves Figure 5 closer to Figure 1. In Figure 5B, the case $N = 1000$ also moves away from Figure 1Y towards Figure 1B, as does the case $N = 1500$. On the other hand, the cases $n = 2000$ and $N = 2500$ in Figure 5B are not close to their counterparts in either Figure 1Y or Figure 1B. This is not unexpected.

The scheme (4.3)–(4.5) is a second-order accurate scheme for (4.2) with general initial data. For the resulting function $u(t, x)$ to solve (1.1), say with initial data

$$u(0, x) = \varphi(x), \quad u_t(0, x) = \psi(x), \tag{4.6}$$

we need the compatibility condition

$$v(0,x) = \psi(x) + \varphi'(x), \quad w(0,x) = \psi(x) - \varphi'(x). \tag{4.7}$$

Then (u, v, w) solves the overdetermined system

$$\begin{aligned} v_t - v_x &= f(u), \\ u_t + u_x &= v, \\ w_t + w_x &= f(u), \\ u_t - u_x &= w. \end{aligned} \tag{4.8}$$

We construct a third-order accurate difference scheme by discretizing the following integral equations:

$$\begin{aligned} v(t,x) &= v(t-h, x+h) + \int_0^h f\big(u(t-h+s, x+h-s)\big)\, ds, \\ w(t,x) &= w(t-h, x-h) + \int_0^h f\big(u(t-h+s, x-h+s)\big)\, ds, \\ u(t,x) &= \frac{1}{2}\Big[u(t-h, x-h) + \int_0^h v(t-h+s, x-h+s)\, ds\Big] \\ &\quad + \frac{1}{2}\Big[u(t-h, x+h) + \int_0^t w(t-h+s, x+h-s)\, ds\Big]. \end{aligned} \tag{4.9}$$

The first equation in (4.9) coincides with the formula for $v(t,x)$ in (2.3). The second equation is its counterpart, derived from the third equation of (4.8). The third equation in (4.9) arises from averaging the formula for $u(t,x)$ in (2.3) and its counterpart arising from the fourth equation in (4.8). From (4.9), a third-order accurate scheme is constructed as follows. Set

$$\begin{aligned} v_{jk} &= v_{j-1,k+1} + \frac{h}{6}\big[f(u_{j-1,k+1}) + 4f(\hat{u}_{j-1/2,k+1/2}) + f(\hat{u}_{jk})\big], \\ w_{jk} &= w_{j-1,k-1} + \frac{h}{6}\big[f(u_{j-1,k-1}) + 4f(\hat{u}_{j-1/2,k-1/2}) + f(\hat{u}_{jk})\big], \\ u_{jk} &= \frac{1}{2}(u_{j-1,k-1} + u_{j-1,k+1}) \\ &\quad + \frac{h}{12}(v_{j-1,k-1} + 4\hat{v}_{j-1/2,k-1/2} + v_{jk}) \\ &\quad + \frac{h}{12}(w_{j-1,k+1} + 4\hat{w}_{j-1/2,k+1/2} + w_{jk}). \end{aligned} \tag{4.10}$$

Here the quantities $\hat{u}_{j-1/2,k+1/2}, \hat{u}_{jk}, \hat{u}_{j-1/2,k-1/2}, \hat{v}_{j-1/2,k-1/2}$, and $\hat{w}_{j-1/2,k+1/2}$ are obtained via second-order accurate schemes. We can take

$$\begin{aligned} \hat{u}_{jk} &= \frac{1}{2}(u_{j-1,k-1} + u_{j-1,k+1}) \\ &\quad + \frac{h}{4}\big[v_{j-1,k-1} + v_{j-1,k+1} + w_{j-1,k-1} + w_{j-1,k+1} \\ &\qquad + hf(u_{j-1,k+1}) + hf(u_{j-1,k-1})\big], \end{aligned} \tag{4.11}$$

with analogous formulas for $\hat{u}_{j-1/2,k\pm1/2}$. Also we can take

$$
\begin{aligned}
\hat{v}_{j-1/2,k-1/2} &= v_{j-1,k} + \frac{h}{4}\big[f(u_{j-1,k}) + f(u^a_{j-1/2,k-1/2})\big], \\
\hat{w}_{j-1/2,k+1/2} &= w_{j-1,k} + \frac{h}{4}\big[f(u_{j-1,k}) + f(u^b_{j-1/2,k+1/2})\big],
\end{aligned} \tag{4.12}
$$

with $u^a_{j-1/2,k-1/2}$ and $u^b_{j-1/2,k+1/2}$ given by first-order accurate schemes, e.g.,

$$
\begin{aligned}
u^a_{j-1/2,k-1/2} &= \frac{1}{2}\Big(u_{j-1,k-1} + u_{j-1,k} + \frac{h}{2}v_{j-1,k-1} + \frac{h}{2}w_{j-1,k}\Big), \\
u^b_{j-1/2,k+1/2} &= \frac{1}{2}\Big(u_{j-1,k} + u_{j-1,k+1} + \frac{h}{2}v_{j-1,k} + \frac{h}{2}w_{j-1,k+1}\Big).
\end{aligned} \tag{4.13}
$$

Results of running this scheme when $f(u) = (1-u^2)(1+4u)$ are presented in Figures 5C and 5D. The graphs in Figure 5C are indistinguishable from those of Figure 1, and the graphs in Figure 5D are indistinguishable from those of Figure 1B, through $N = 1500$; again they diverge for $N = 2000$ and 2500.

Figures 6A–6C deal with $f(u) = u - u^3$, to be compared with Figures 4B, 4C, 4Y, and 4Z. The cases where $N = 500$ in Figures 6A and 6B look indistinguishable from that in Figure 4B, and in particular the second-order accurate scheme used in Figure 6A slightly improves on the picture in Figure 4Y. A similar remark can be made about the case $N = 1500$. For $N = 2000$, Figure 6B looks just like Figure 4B, while Figure 6A has deviated, though arguably not as much as Figure 4Y. A similar remark can be made for the case $N = 2500$. As for Figure 6C, it matches Figure 4C perfectly through $N = 4000$, though once bilateral symmetry is lost in Figure 4C, the pictures diverge completely, even at $N = 6000$.

One result suggested by these pictures is that enforcing the flip symmetry (4.1) seems to produce a better second-order accurate scheme than was produced in §2. One would guess the third-order accurate scheme (4.10)–(4.13) also produces better output than is given by (2.7)–(2.9).

However we have encountered some remarkable anomalies in the seemingly innocuous cases $f(u) = -\sin u$ and $f(u) = -u - u^3$, for moderately large N. See Figure 7 for a solution to $u_{tt} = u_{xx} - \sin u$, computed for $N \le 10000$ via (4.10)–(4.13). The pictures match up perfectly with those of Figure 2C, through $N = 6000$. At $N = 8000$ the difference is almost imperceptible, but in fact an instability is just beginning at this point. From here on the graph produced by u_{jk} splits into two, one for k even and one for k odd, and proceeds to the mess at $N = 10000$ shown in the last picture of Figure 7. The bilateral symmetry forces $u_{j0} = u_{j1}$, so the two curves are tied together at the endpoints. For $f(u) = -u - u^3$, such an instability has its onset slightly before $N = 6000$, as shown in Figure 8. As seen in Figure 7B, the second-order accurate scheme (4.3)–(4.5) does not produce this instability, at least not for $N \le 10000$. Also, as already seen in Figure 6C, the third-order accurate scheme (4.10)–(4.13) does not produce such an instability (at least for $N \le 10000$) in the apparently more turbulent case $f(u) = u - u^3$. This leaves us with a fine mystery, to understand this slow instability.

Finally we make contact with the popular centered difference scheme

$$u_{j+1,k} = 2u_{jk} - u_{j-1,k} + \alpha^2(u_{j,k-1} - 2u_{jk} + u_{j,k+1}) + (\alpha h)^2 f(u_{jk}), \tag{4.14}$$

which also enforces the flip symmetry (4.1). Here $u_{jk} = u(j\alpha h, kh)$ approximates $u(t,x)$. The Lewy condition requires $\alpha \in (0,1]$. We apply this to the case (3.2). In Figure 5CD we take $\alpha = 1$ and show graphs with $N \le 500$, which match up perfectly with graphs in Figures 1, 1X, 5, and 5C. In Figure 5CD2 we show this suffers an instability at $N \approx 800$, of a nature similar to that at $N \approx 10000$ in Figure 7 and at $N \approx 6000$ in Figure 8. In Figure 5CD3 we implement (4.14) with $\alpha = 1/2$. Thus each iteration of (4.14) corresponds to $1/2$ a unit of time, so $2N$ iterations are used in each graph, with label $N = 500,\ 1000$, etc. We see that the graphs in Figures 5CD3 match up with those generated by third-order accurate schemes in Figures 1B and 5D, up through $N = 1000$, but diverge at $N = 1500$, while the graphs in Figures 1B and 5D remain identical through $N = 1500$. This is an indication that the third-order schemes remain accurate beyond the point at which the scheme (4.14) loses its accuracy, for the case (3.2). Further graphs, not presented here, indicate that the result of (4.14) starts to diverge from these third-order accurate schemes at $N \approx 1200$, while the two third-order accurate schemes start to diverge from each other at $N \approx 1700$. This indicates the degree to which output from (4.14) is not as accurate as output from our third-order accurate schemes. By the way, output from the second-order accurate scheme (4.3)–(4.5) slightly differs from these other graphs at $N = 1100$ and differs more than that of (4.14) at $N = 1200$, so (4.14) seems to perform slightly better than this other second-order accurate scheme.

A similar story regarding $f(u) = u - u^3$ is indicated in Figures 6CD and 6CD2.

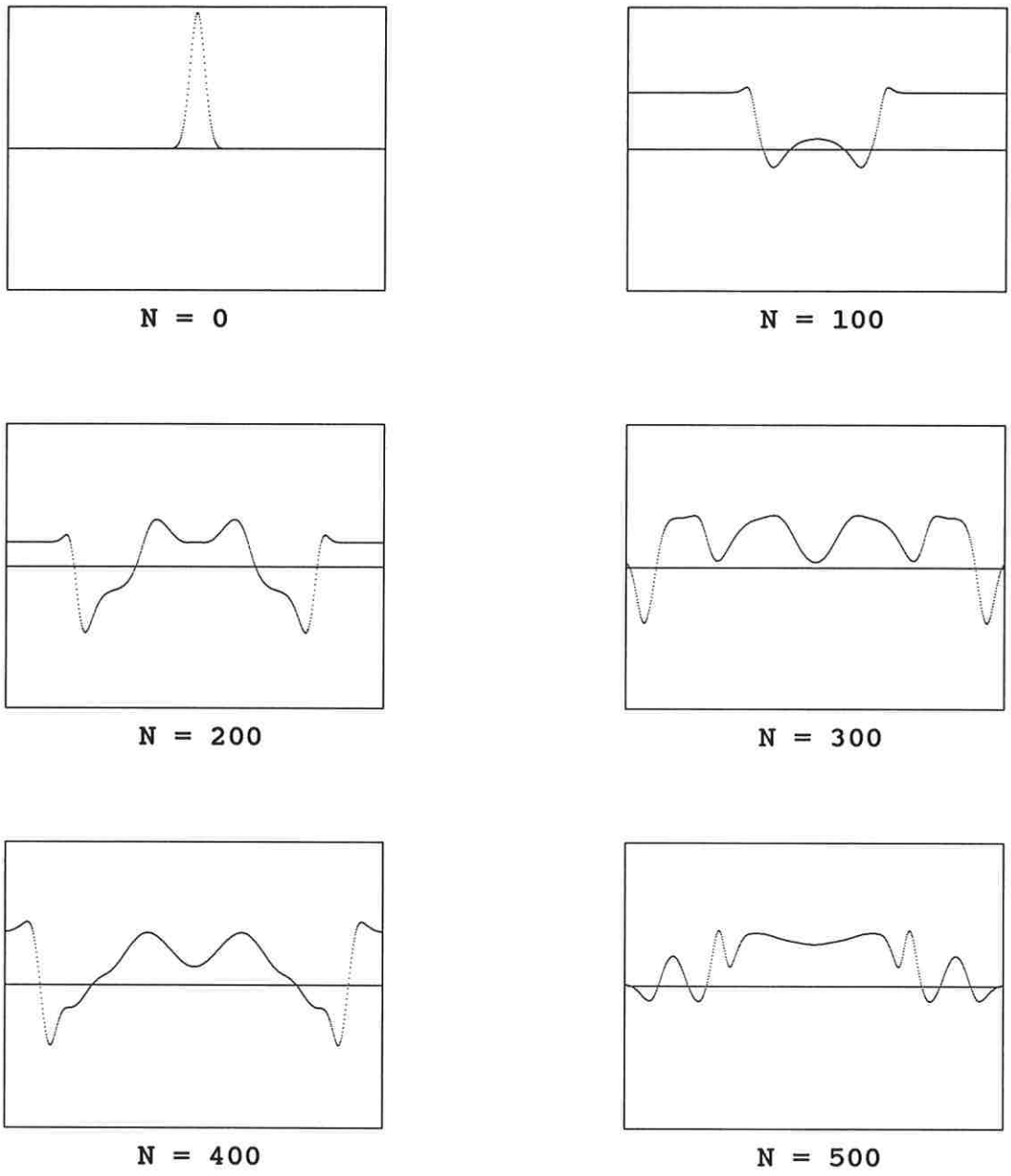

Figure 5

Solution to $u_{tt} = u_{xx} + (1 - u^2)(1 + 4u)$

Second Order Accurate Scheme, Bilateral Symmetry Enforced

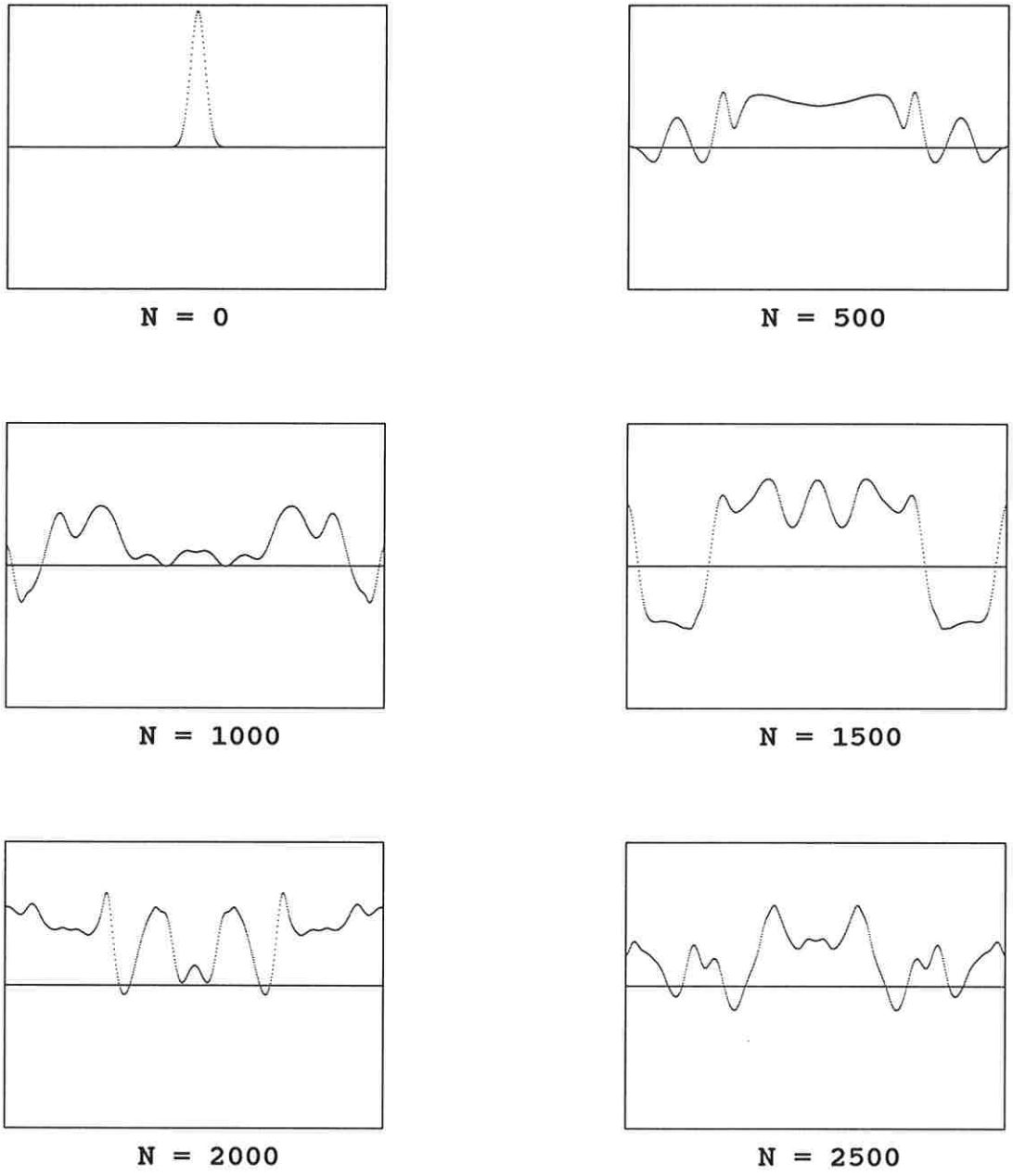

Figure 5B

Solution to $u_{tt} = u_{xx} + (1 - u^2)(1 + 4u)$

Second Order Accurate Scheme, Bilateral Symmetry Enforced

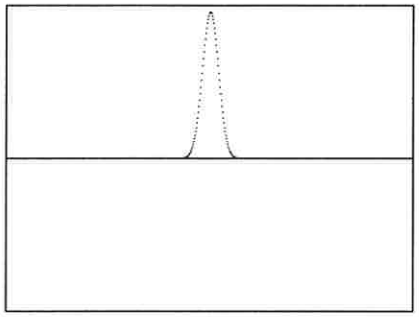

N = 0

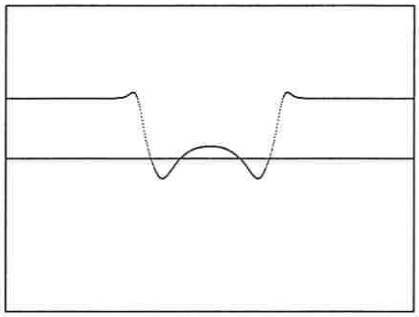

N = 100

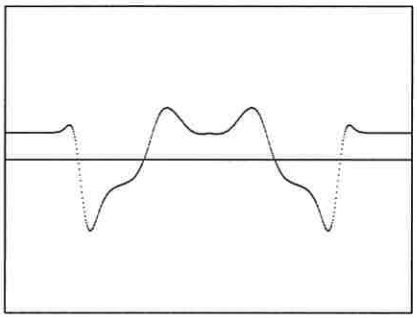

N = 200

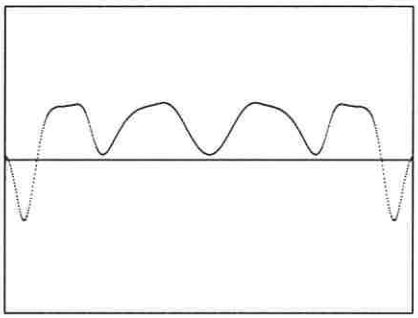

N = 300

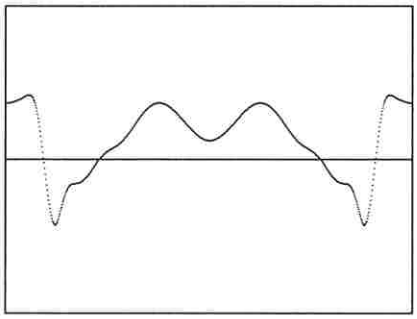

N = 400

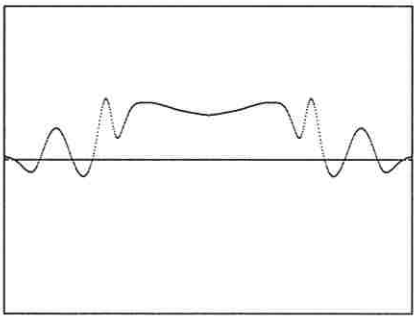

N = 500

Figure 5CD

Solution to $u_{tt} = u_{xx} + (1 - u^2)(1 + 4u)$

Centered Difference Scheme

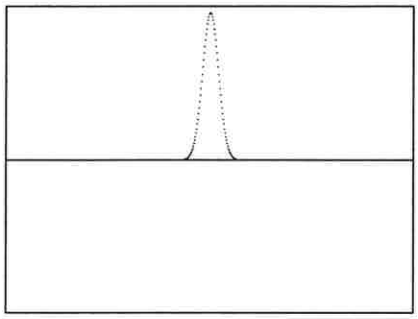

N = 0

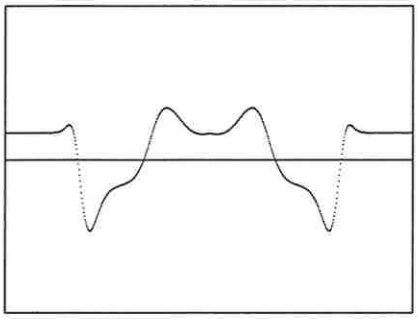

N = 200

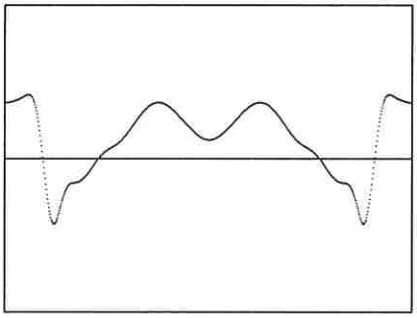

N = 400

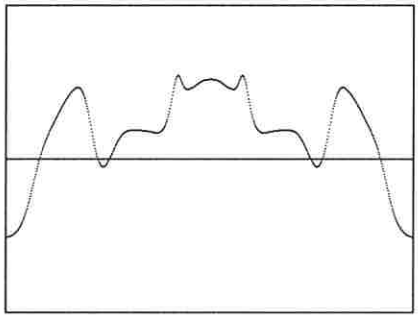

N = 600

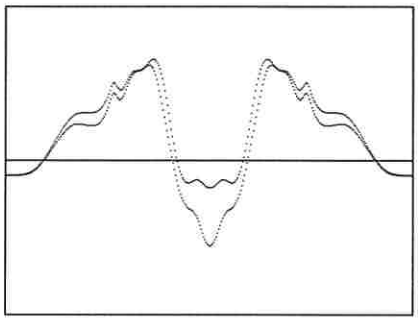

N = 800

Figure 5CD2

Solution to $u_{tt} = u_{xx} + (1 - u^2)(1 + 4u)$

Centered Difference Scheme
Instability Around $N = 800$

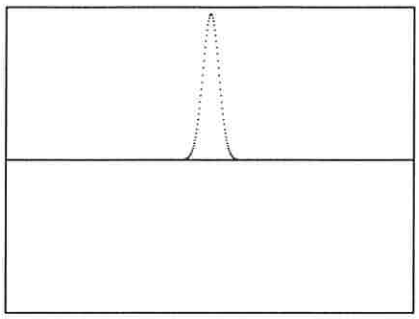

N = 0

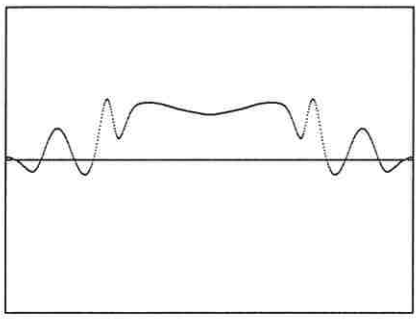

N = 500

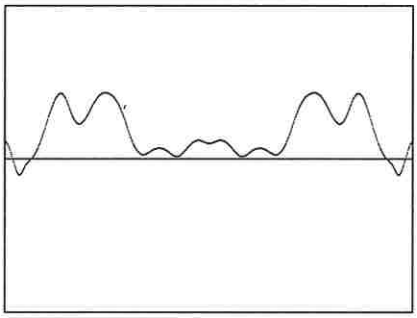

N = 1000

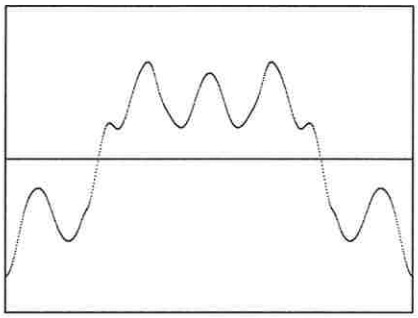

N = 1500

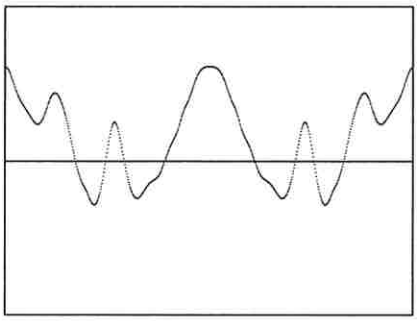

N = 2000

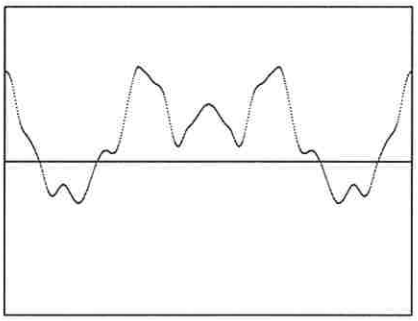

N = 2500

Figure 5CD3

Solution to $u_{tt} = u_{xx} + (1 - u^2)(1 + 4u)$

Centered Difference Scheme

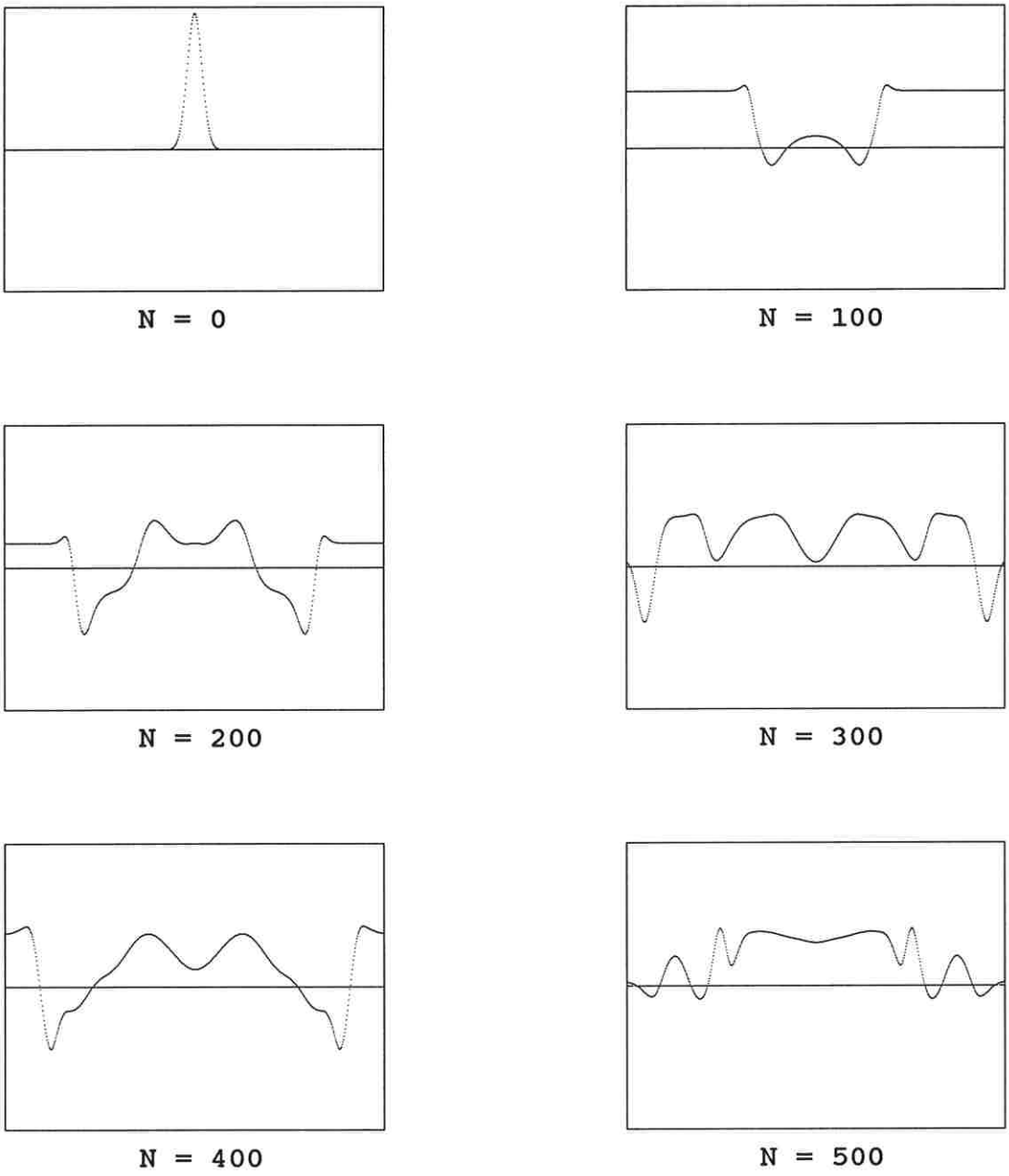

Figure 5C

Solution to $u_{tt} = u_{xx} + (1 - u^2)(1 + 4u)$

Third Order Accurate Scheme, Bilateral Symmetry Enforced

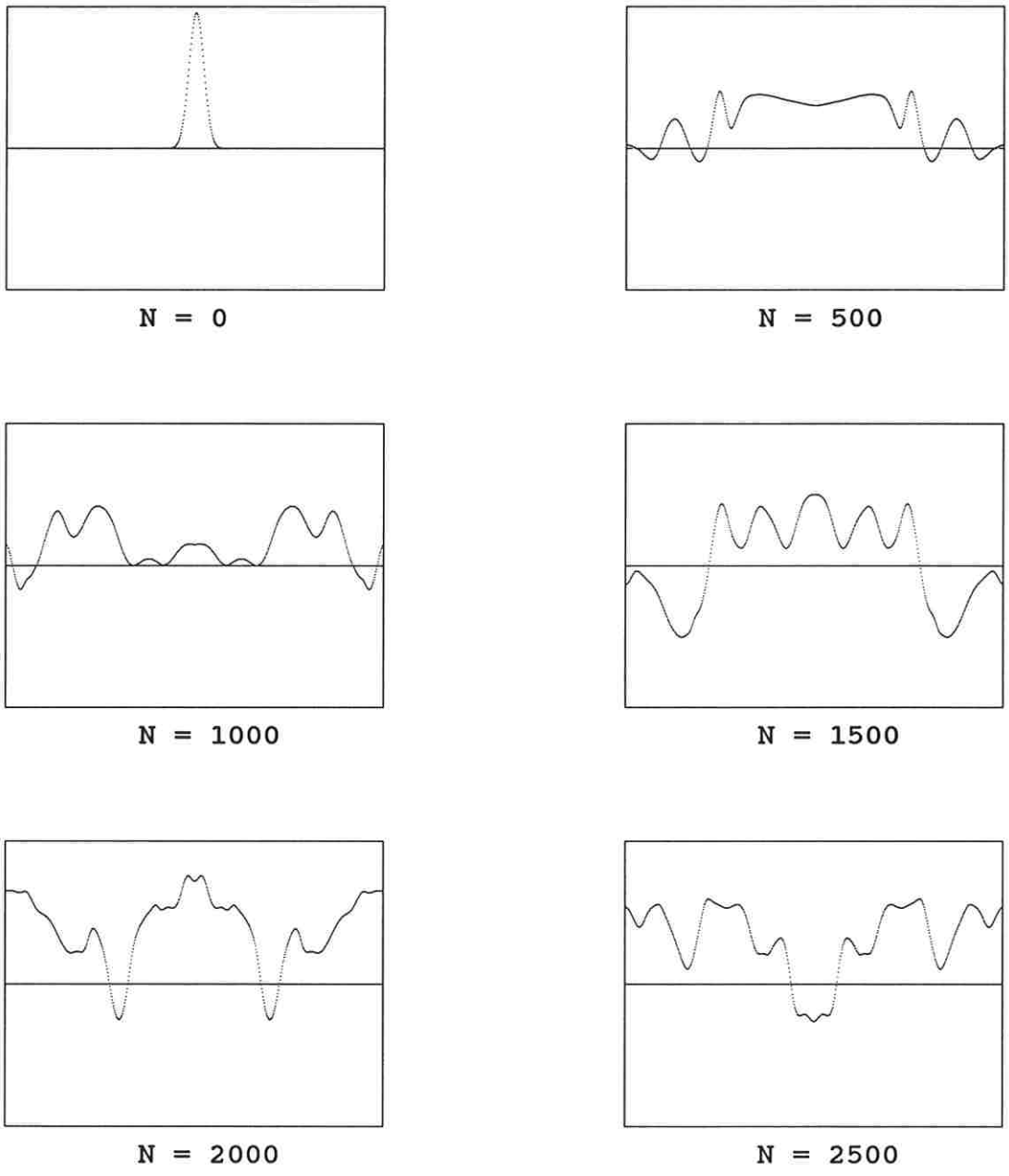

Figure 5D

Solution to $u_{tt} = u_{xx} + (1 - u^2)(1 + 4u)$

Third Order Accurate Scheme, Bilateral Symmetry Enforced

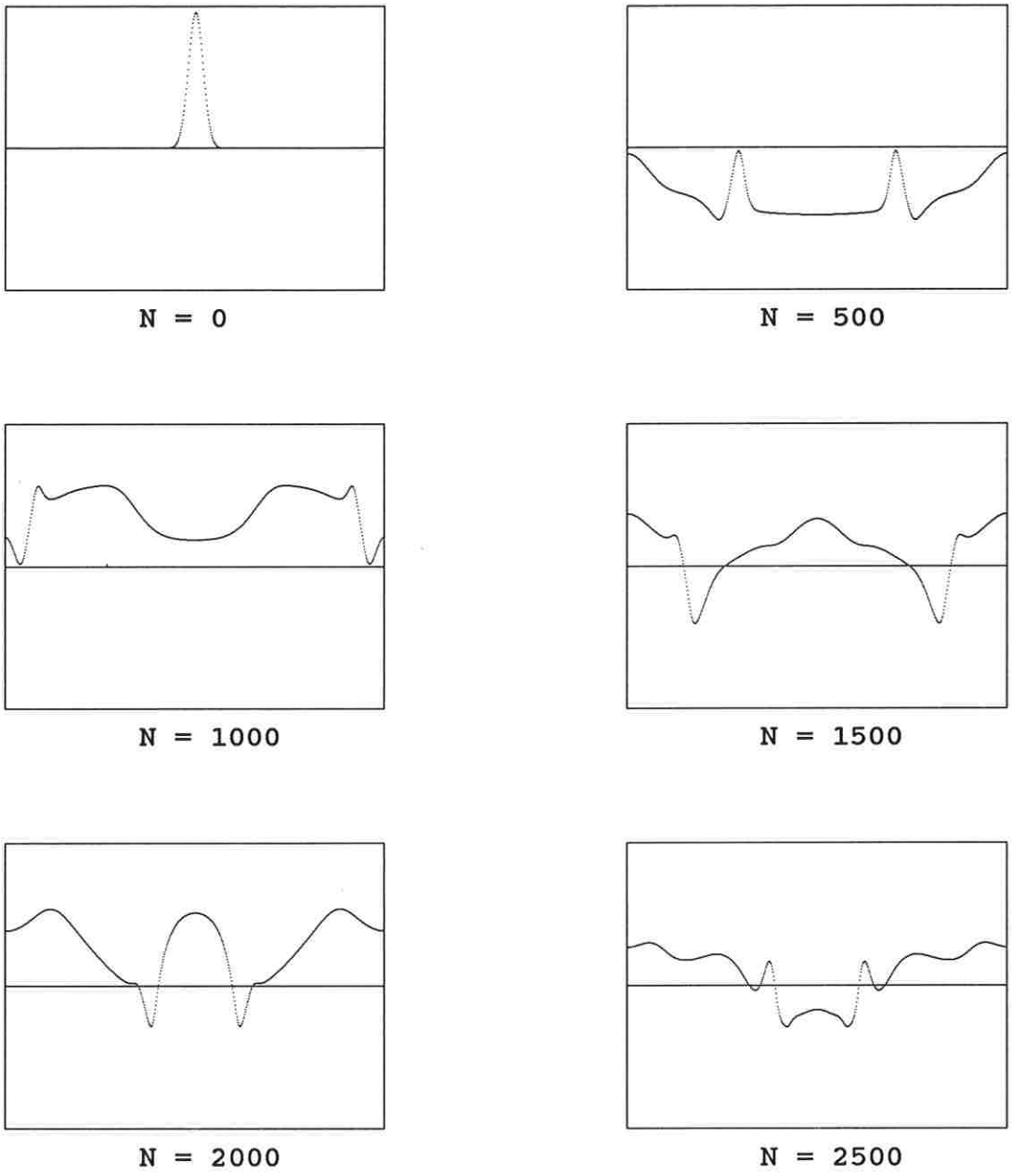

Figure 6A

Solution to $u_{tt} = u_{xx} + u - u^3$

Second Order Accurate Scheme, Bilateral Symmetry Enforced

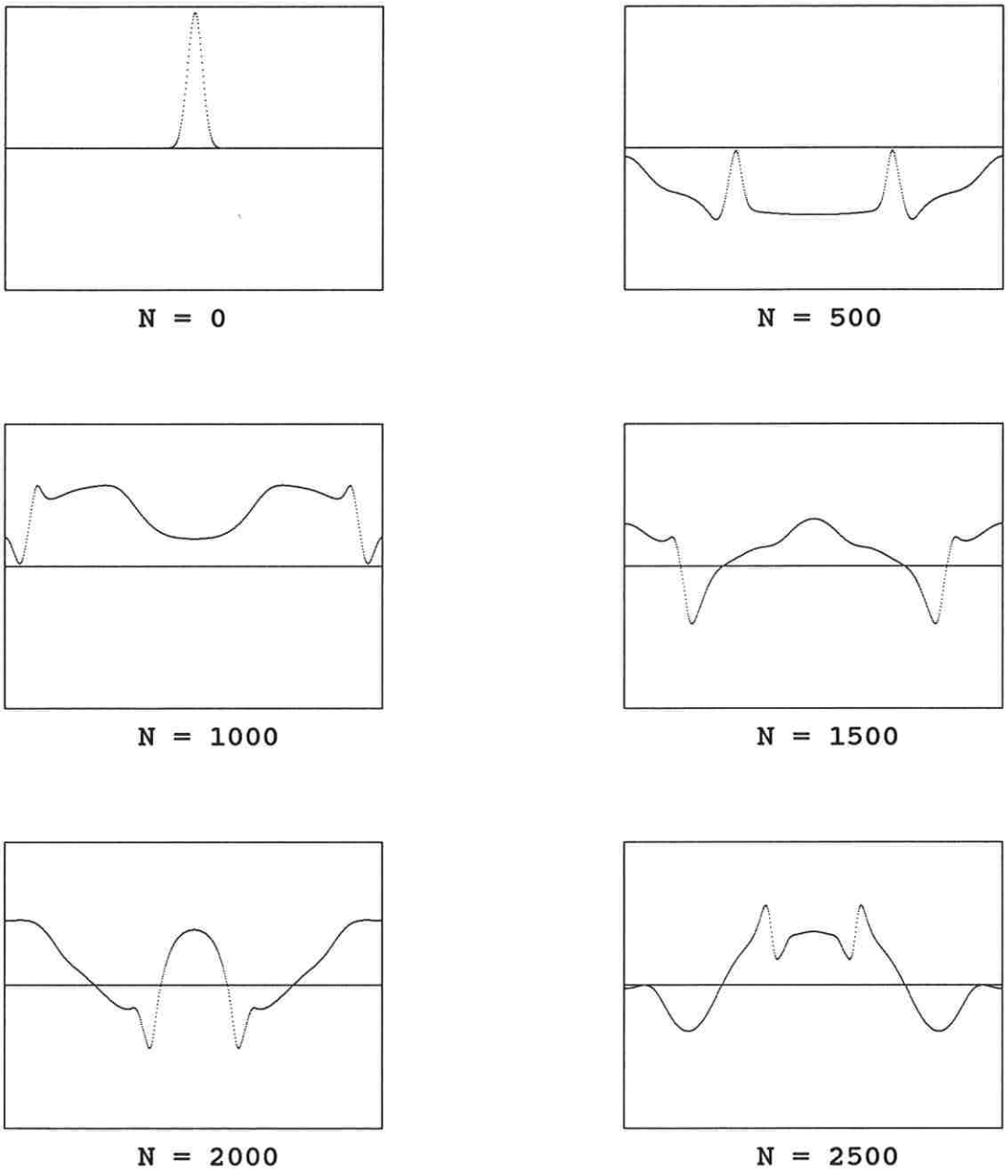

Figure 6B

Solution to $u_{tt} = u_{xx} + u - u^3$

Third Order Accurate Scheme, Bilateral Symmetry Enforced

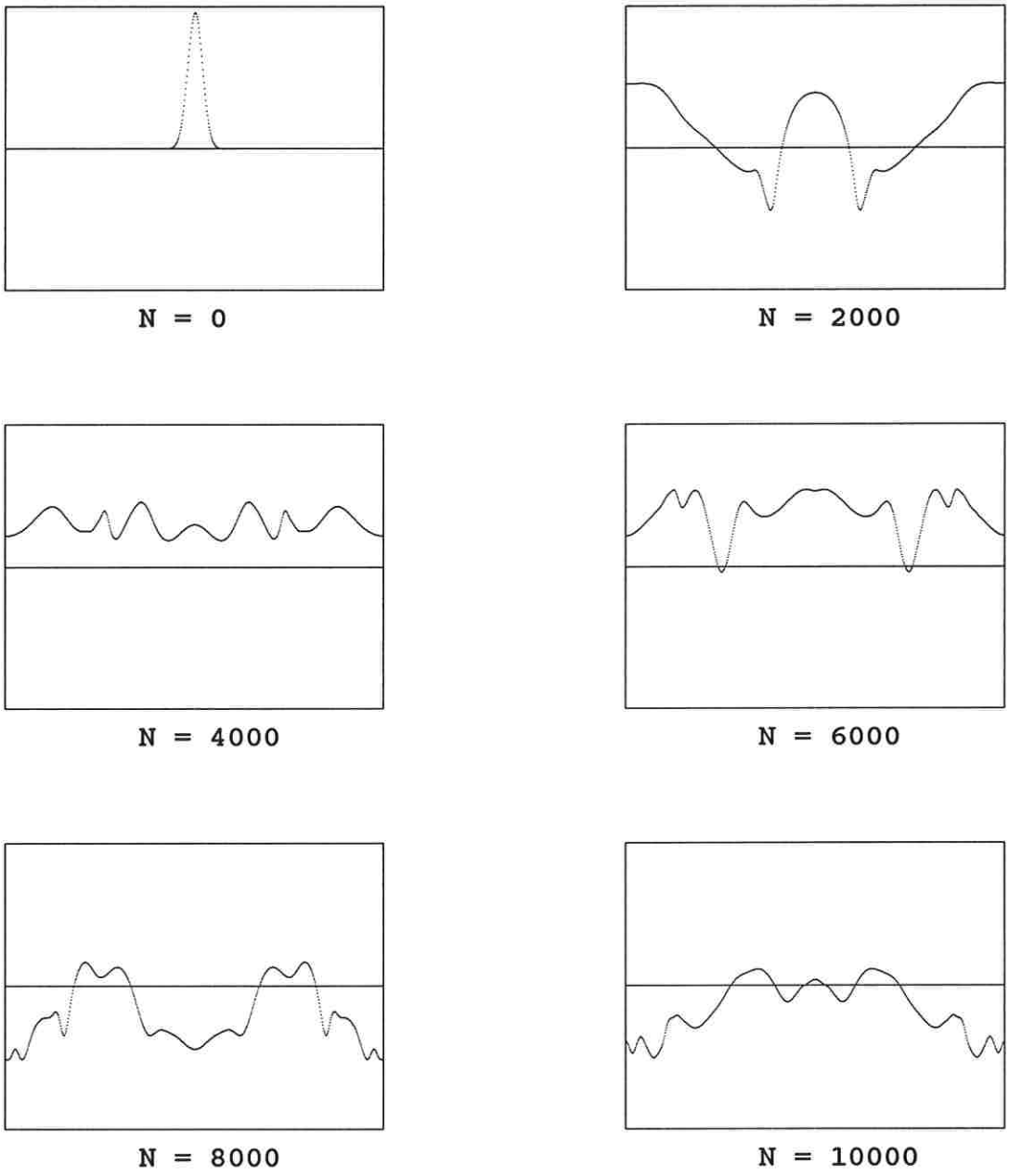

Figure 6C

Solution to $u_{tt} = u_{xx} + u - u^3$

Third Order Accurate Scheme, Bilateral Symmetry Enforced

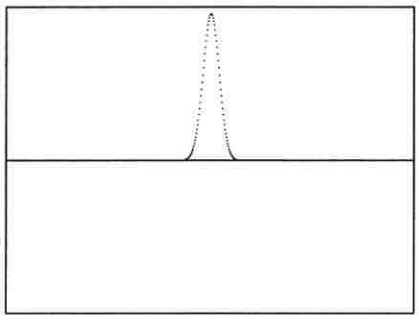

N = 0

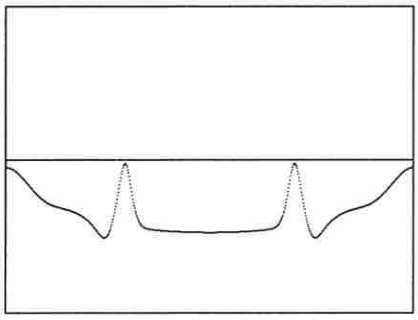

N = 500

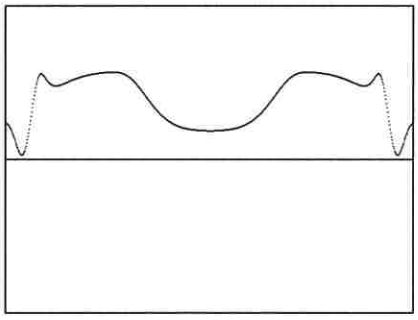

N = 1000

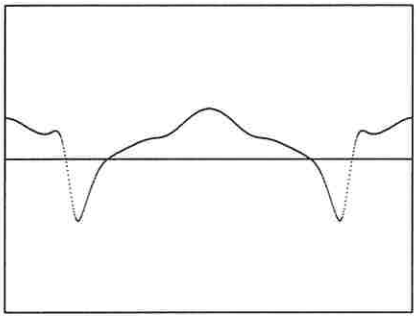

N = 1500

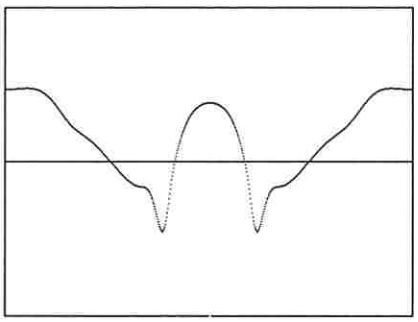

N = 2000

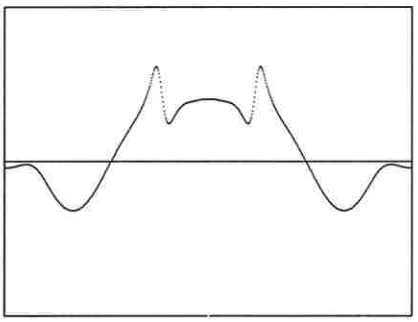

N = 2500

Figure 6CD

Solution to $u_{tt} = u_{xx} + u - u^3$

Centered Difference Scheme

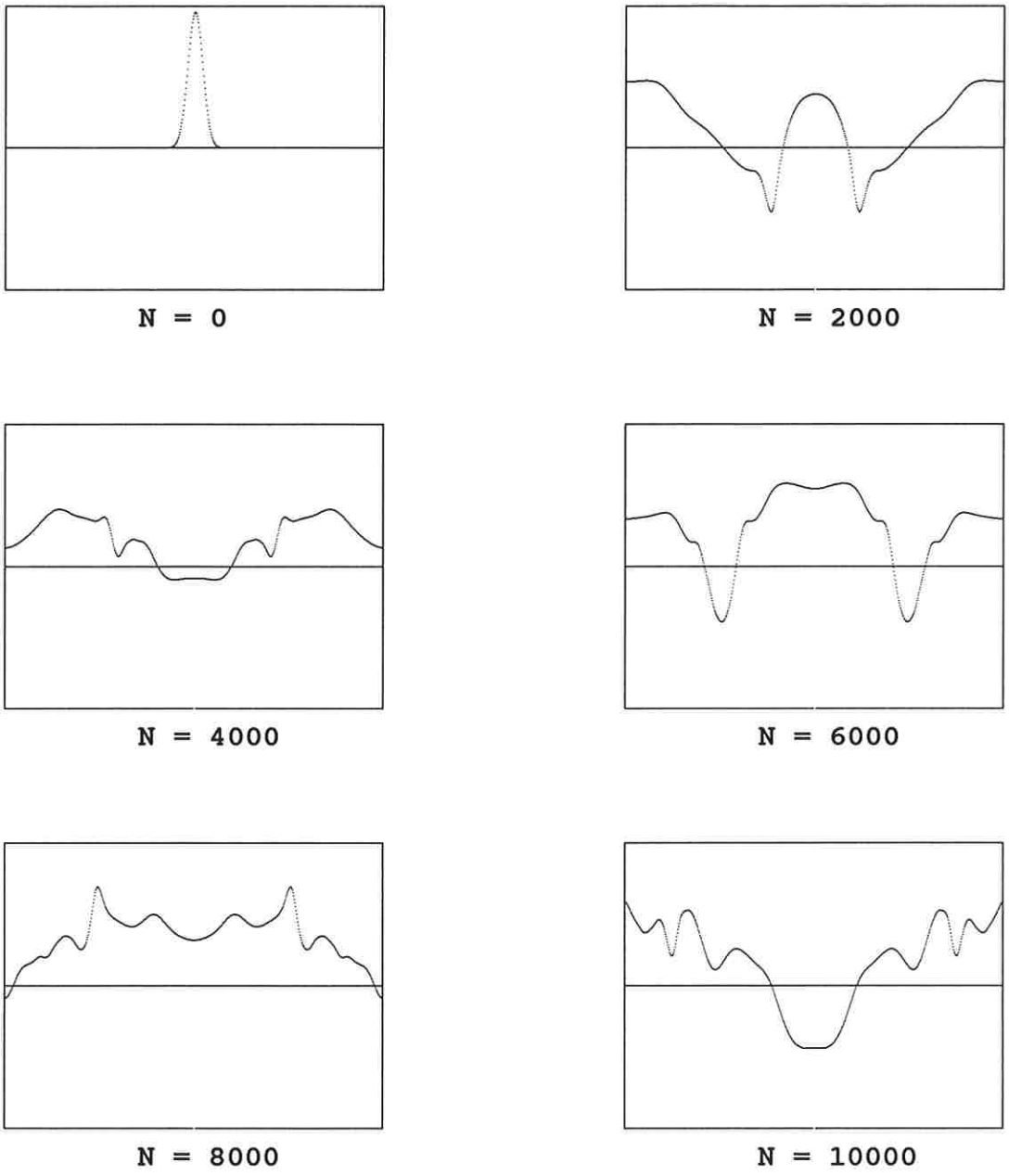

Figure 6CD2

Solution to $u_{tt} = u_{xx} + u - u^3$

Centered Difference Scheme

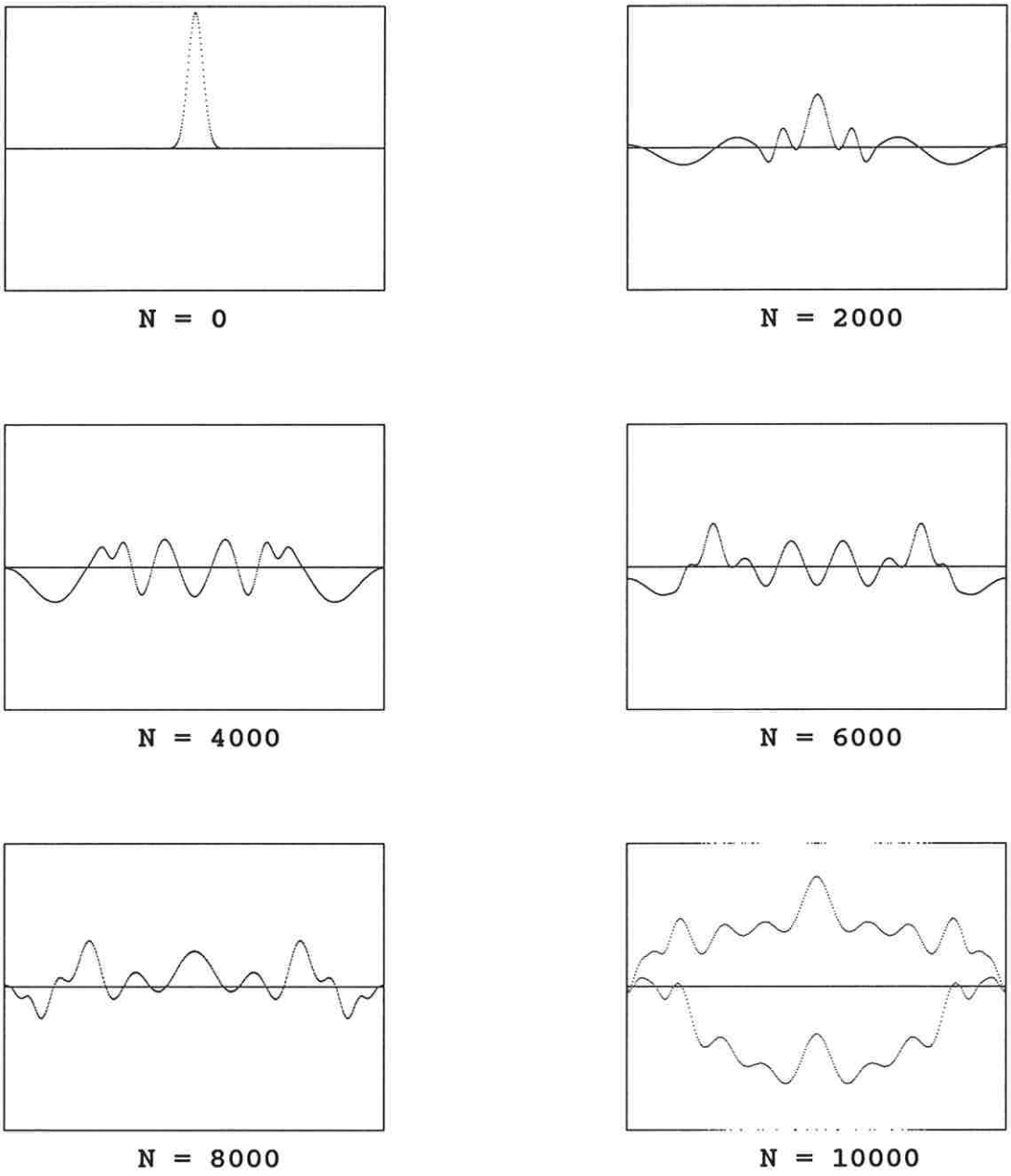

Figure 7

Solution to $u_{tt} = u_{xx} - \sin u$

Third Order Accurate Scheme, Bilateral Symmetry Enforced
Strange Behavior Incipient Around N = 8000

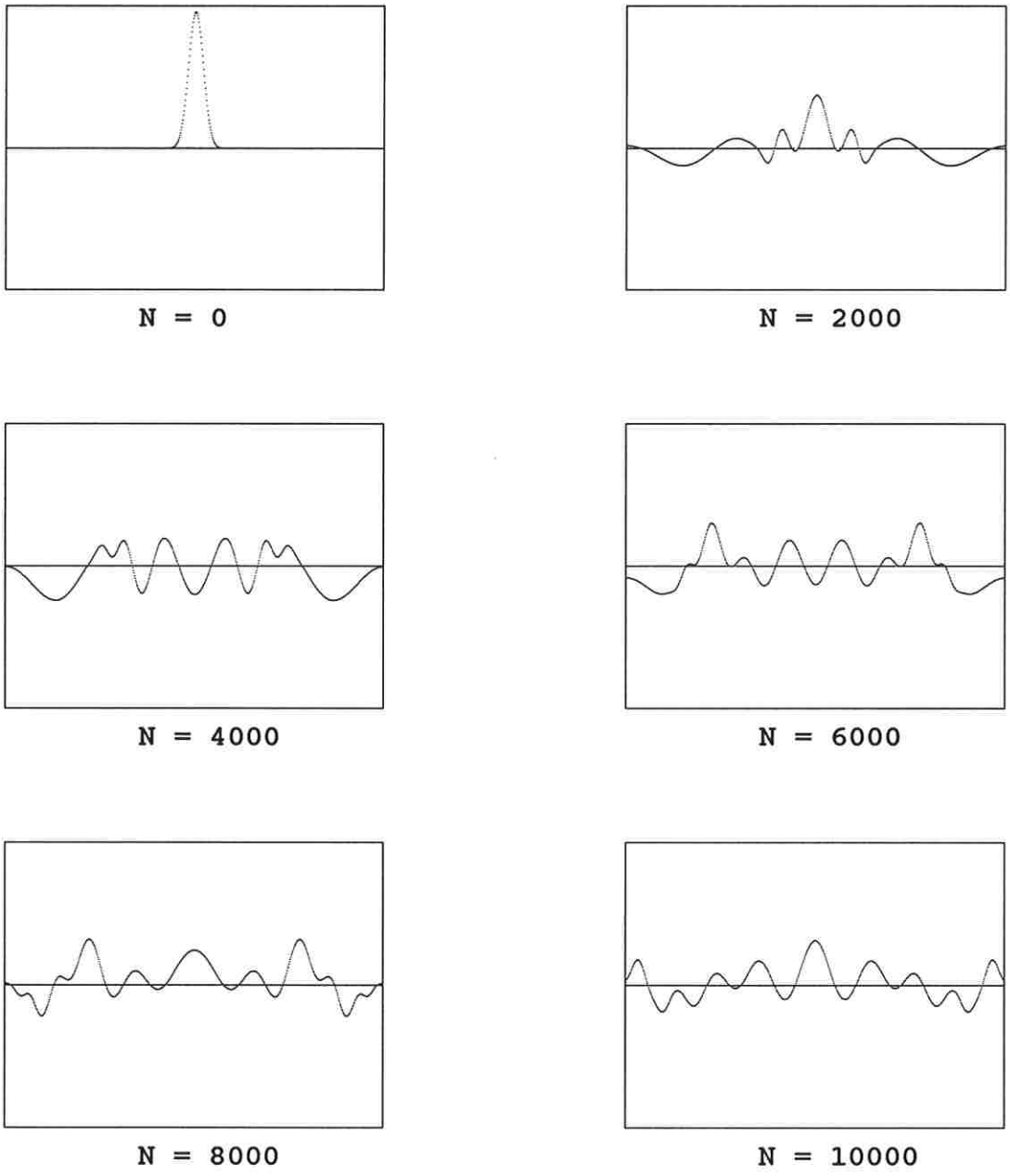

Figure 7B

Solution to $u_{tt} = u_{xx} - \sin u$

Second Order Accurate Scheme, Bilateral Symmetry Enforced

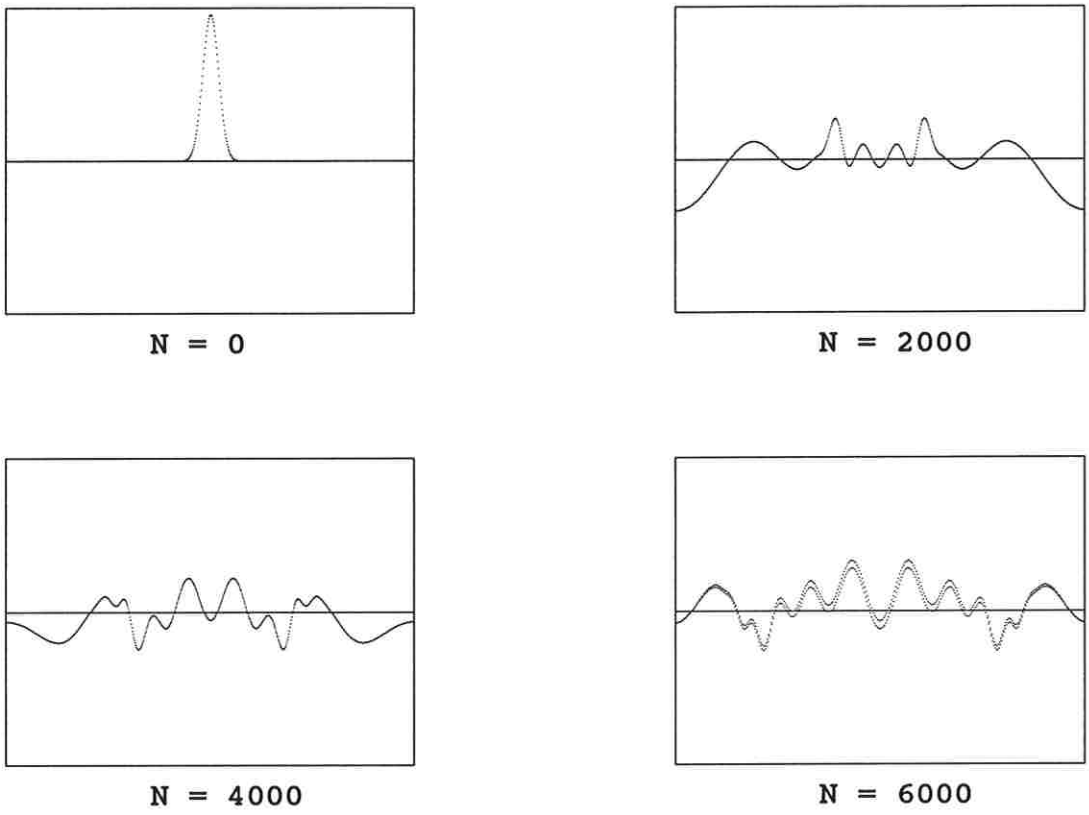

Figure 8

Solution to $u_{tt} = u_{xx} - u - u^3$

Third Order Accurate Scheme, Bilateral Symmetry Enforced
Strange Behavior Incipient Around N = 6000

5. Wave patterns

Here we present pictures of wave patterns formed by solutions to

$$u_{tt} = u_{xx} + f(u), \tag{5.1}$$

in various cases, starting with Figures 9A–9D, where

$$f(u) = c^2(1-u^2)(1+4u), \tag{5.2}$$

with $c^2 = 1, 2.5, 3.5$, and 5, respectively. Note that if $u(t,x)$ solves (5.1) and $u^c(t,x) = u(ct,cx)$, then u^c solves

$$u^c_{tt} = u^c_{xx} + c^2 f(u^c), \tag{5.3}$$

so solutions to (5.3) are scaled versions of solutions to (5.1) (though the initial data are altered). In all cases here we take

$$u(0,x) = 2.3\, e^{-16x^2}, \quad u_t(0,x) = 0. \tag{5.4}$$

We use the third-order accurate scheme (2.7)–(2.9), with $h = 0.02$. We periodize, so $u(t,x)$ is periodic in x of period 1899/50. More precisely, $u(t,x)$ is approximated by $u(jh,(k-950)h) = u_{jk}$, and u_{jk} is periodic in k of period 1899. In most pictures we produce the pattern of the wave $u(t,x)$ for $0 \le j \le 1200$, i.e., for $0 \le t \le 24$. We impose bilateral symmetry cheaply, by taking data from u_{jk} only for $0 \le j \le 950$ and reflecting it. (The qualitative results are not that far off from the use of (4.10)–(4.13).)

Figures 9A–9D show substantial complexity. Do these figures, particularly Figures 9C–9D, behave like class 4 cellular automata? This is a question we must leave to the reader, whom we invite to study them closely. What do you see?

For $j \le 940$, the waves are outgoing from the center, but then they meet at $k = 0 \equiv 1899$ and waves moving to the right interact with waves moving to the left. These interactions appear in Figures 9A–9D only in the lower corners. We do not show many pictures here in which such interactions are emphasized, but we do present two, Figure 9A3 and Figure 9BB3, showing wave patterns with $2400 < j \le 3600$ (i.e., $48 < t \le 72$), in which such wave interactions can be seen.

Figures 10A–10D deal with various cases in which $f(0) = 0$. The behavior in Figures 10A-10B is much simpler than in Figures 9A–9D, and it is tempting to speculate that the motion outside the light cone in Figures 9A–9D drives the complex behavior observed there, by scattering in waves that interact with those emanating from the source within the light cone. A suggestion of another mechanism exciting complex behavior can be seen in Figures 10C–10D, though these patterns still seem less complex than those of Figures 9A–9D. This is something that bears further exploration.

Figures 11A–11D deal with various cases in which $f(0) \neq 0$, so there is again a driving force outside the light cone, scattering waves inside it. These behaviors are not as complex as those in Figures 9A–9D. In Figures 11C–11D we see behavior that is fairly complex for $j \leq 600$ or so, and then seems to simplify.

Our last set of wave patterns is presented in Figures 12A–12D, where we take

$$f(u) = c^2(1 + 4\sin u)\cos u, \tag{5.5}$$

with c^2 as described after (5.2). Here we see complex variants of the patterns in Figures 9A–9D, whose further examination is likely to be as intriguing as it should be entertaining.

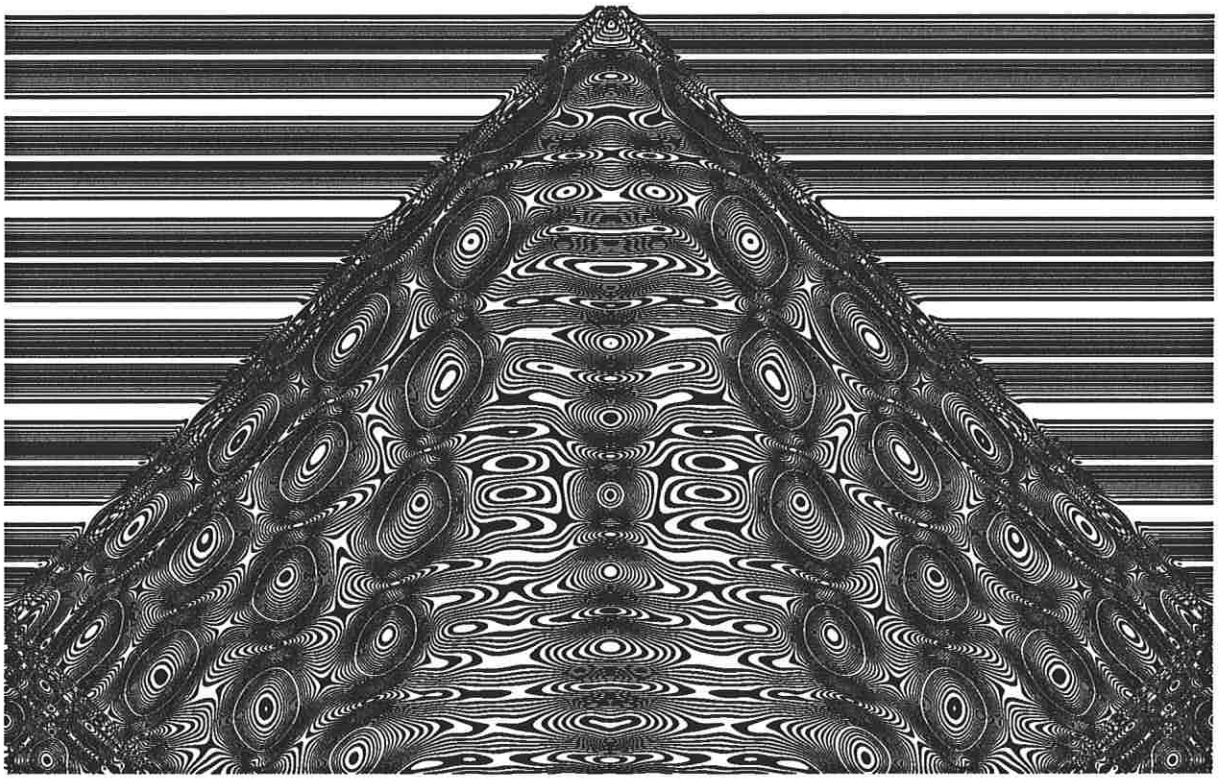

Figure 9A

Contours of Solution to

$$u_{tt} = u_{xx} + (1 - u^2)(1 + 4u)$$

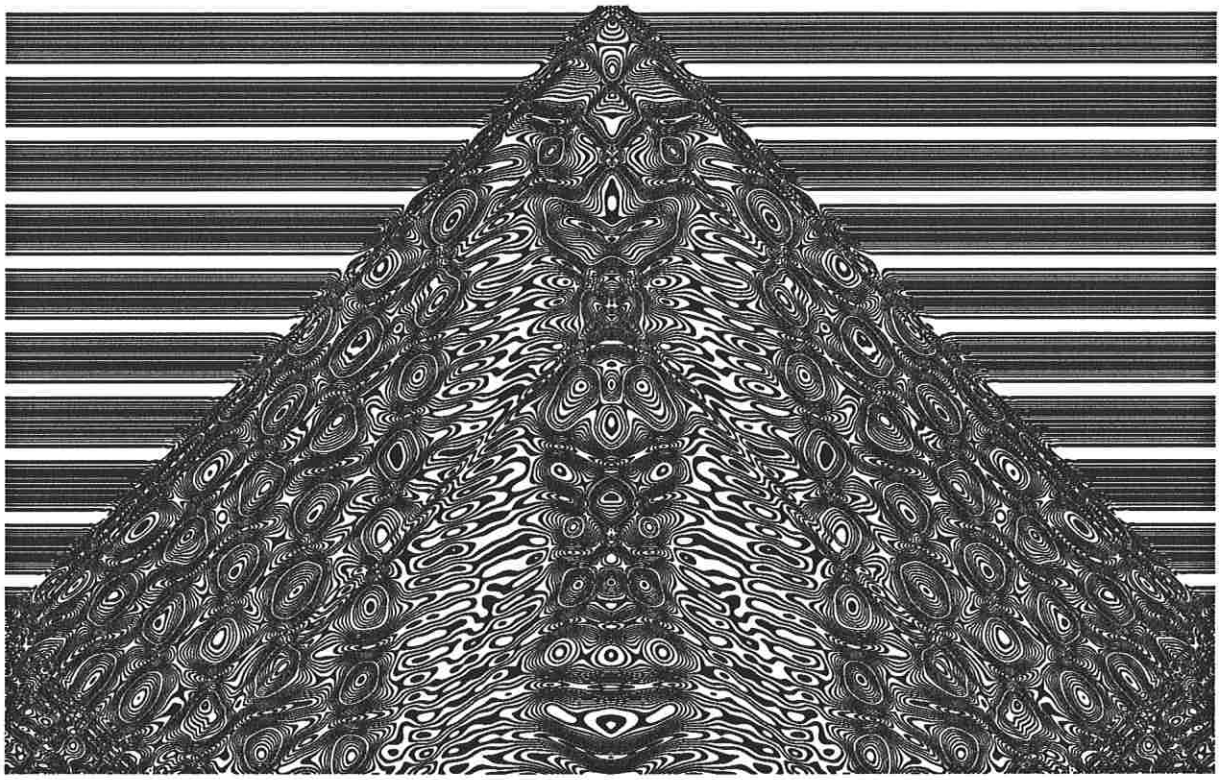

Figure 9B

Contours of Solution to

$$u_{tt} = u_{xx} + \frac{5}{2}(1-u^2)(1+4u)$$

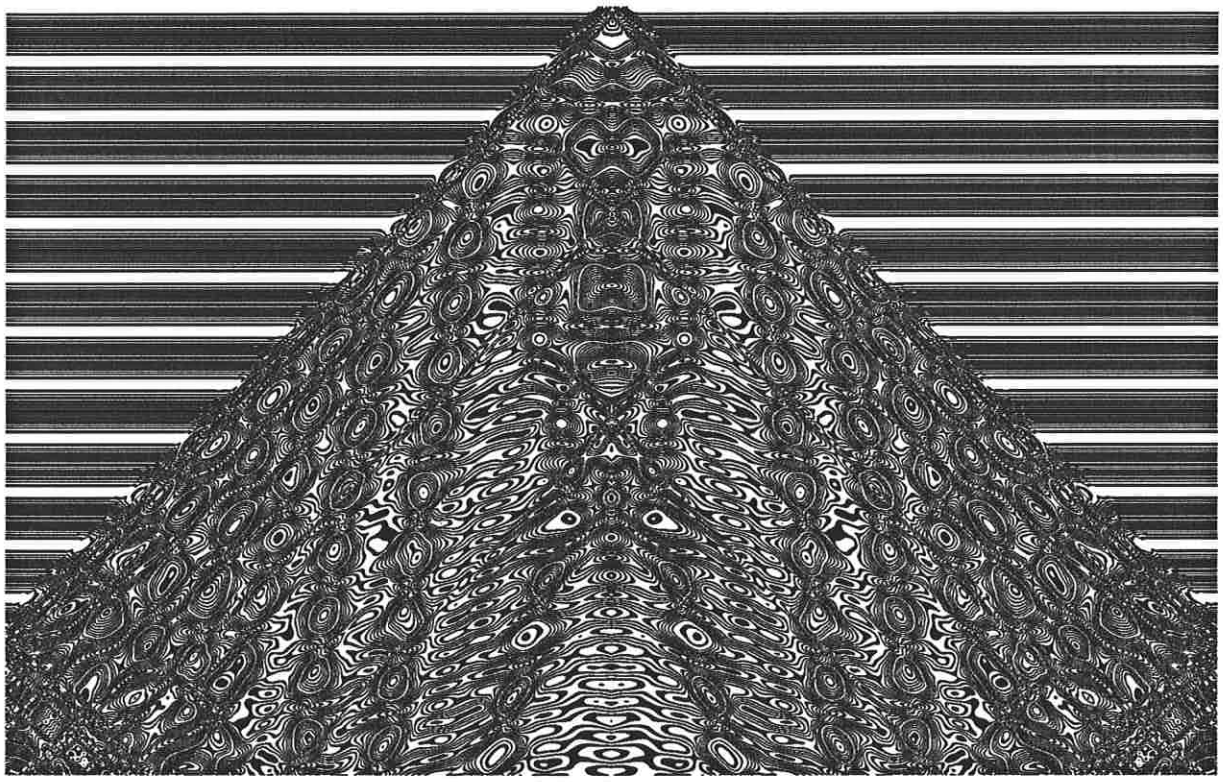

Figure 9C

Contours of Solution to

$$u_{tt} = u_{xx} + \frac{7}{2}(1 - u^2)(1 + 4u)$$

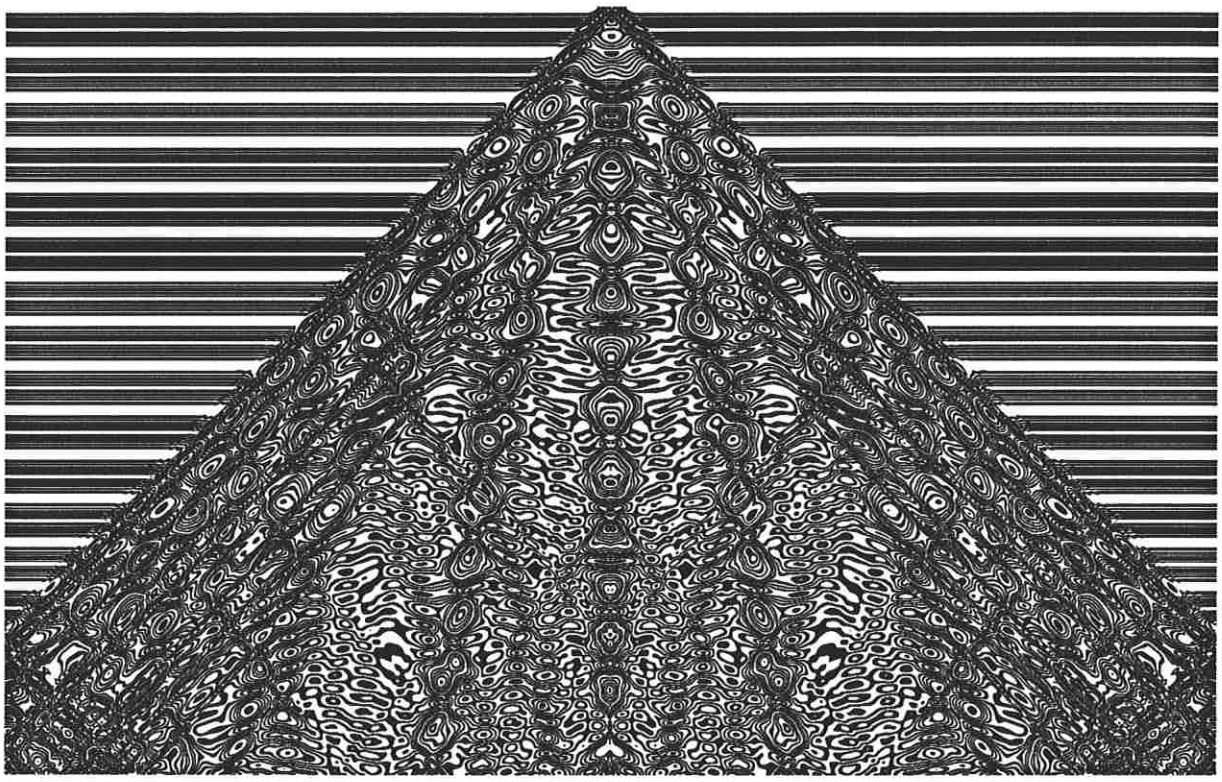

Figure 9D

Contours of Solution to

$$u_{tt} = u_{xx} + 5(1 - u^2)(1 + 4u)$$

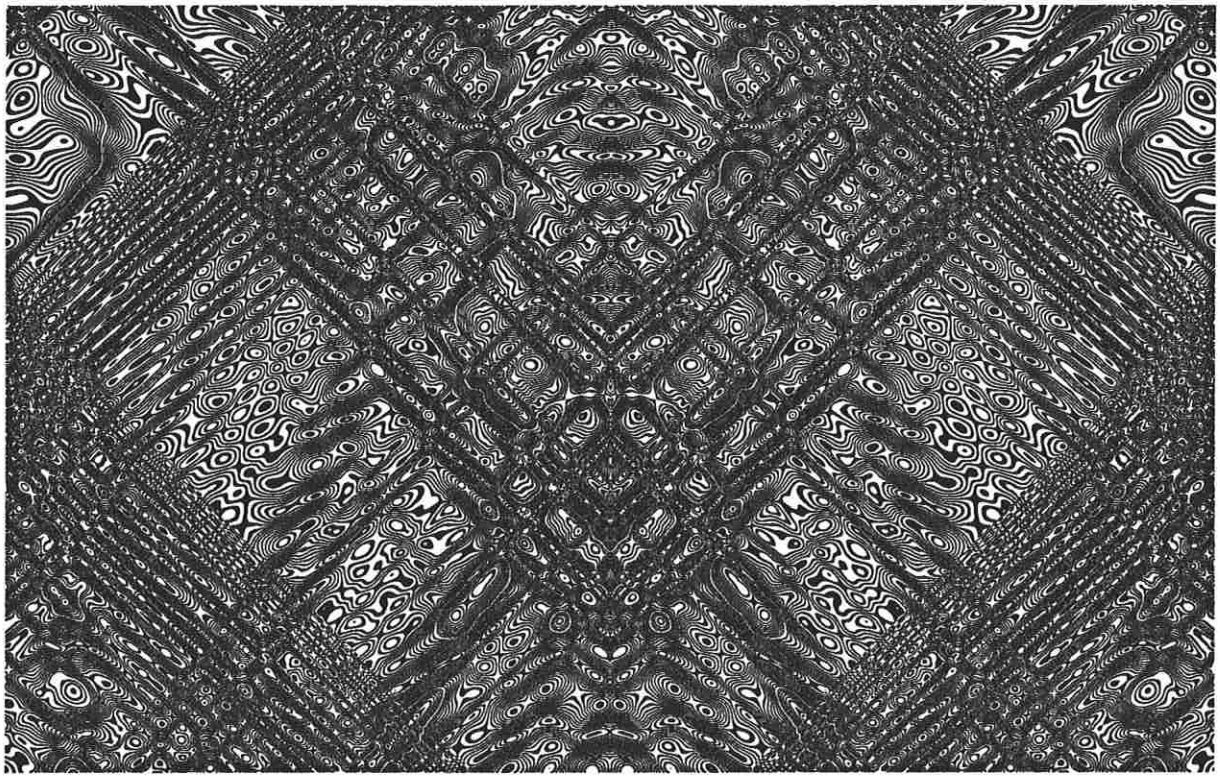

Figure 9A3

Contours of Solution to

$$u_{tt} = u_{xx} + (1 - u^2)(1 + 4u)$$

$$2401 \leq N \leq 3600$$

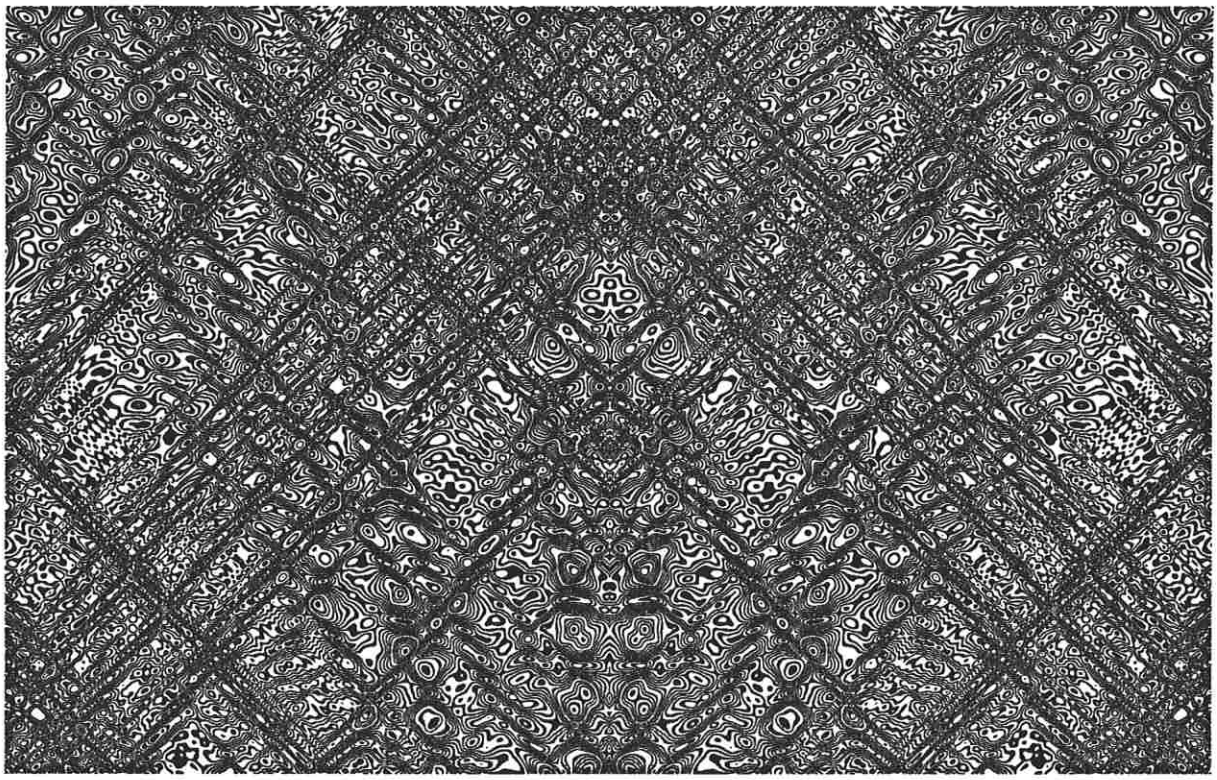

Figure 9BB3

Contours of Solution to

$$u_{tt} = u_{xx} + \frac{5}{2}(1 - u^2)(1 + 4u)$$

$$2401 \leq N \leq 3600$$

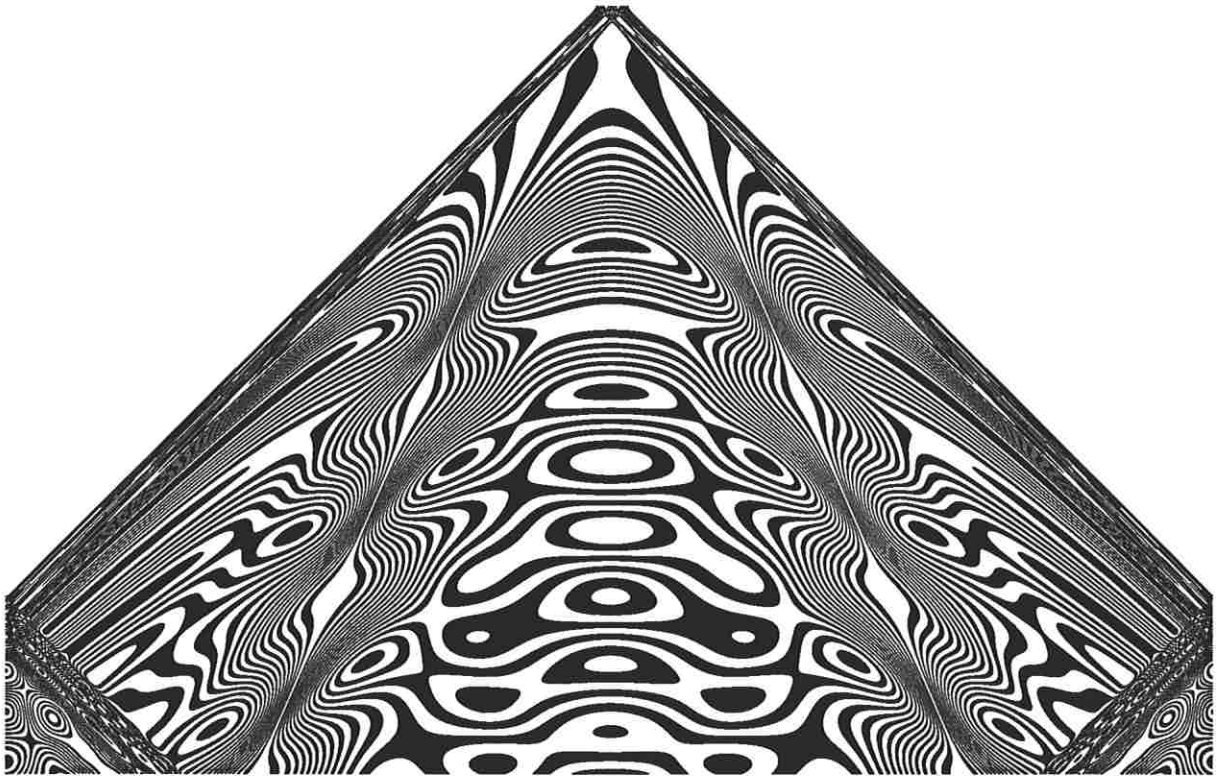

Figure 10A

Contours of Solution to

$$u_{tt} = u_{xx} + u - u^3$$

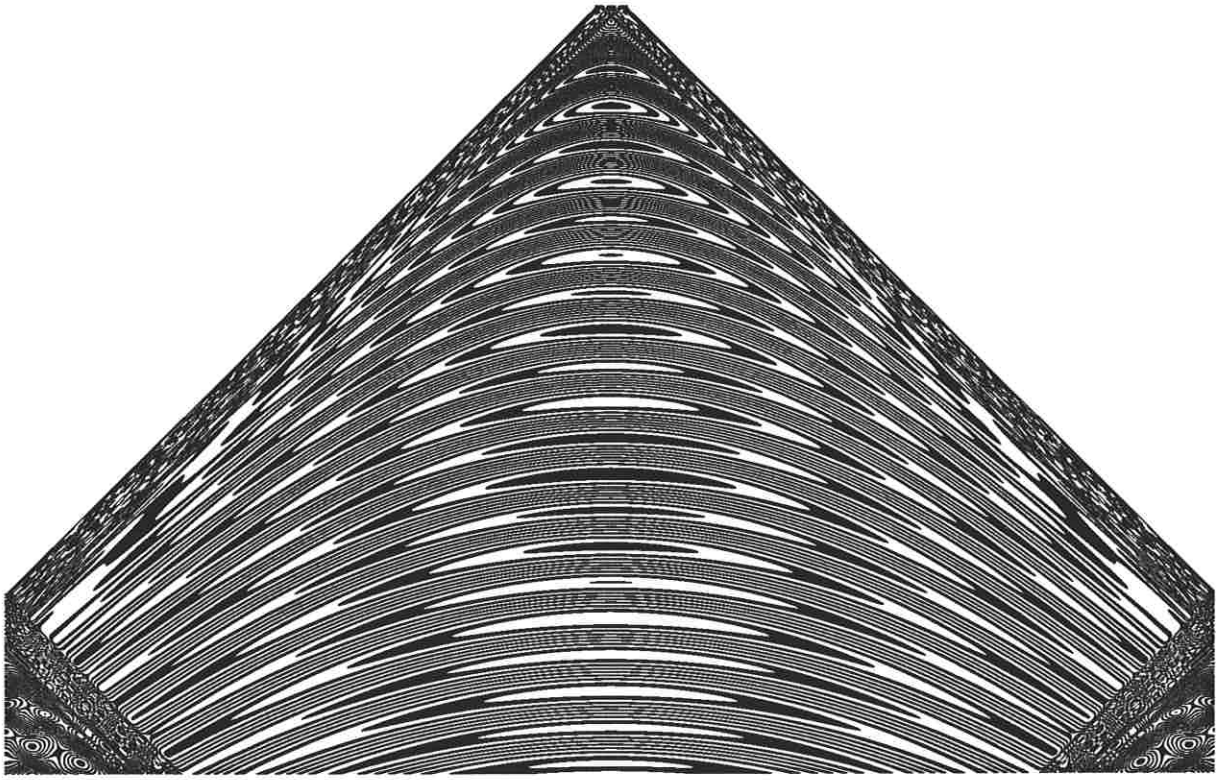

Figure 10B

Contours of Solution to

$$u_{tt} = u_{xx} + 4u - u^3$$

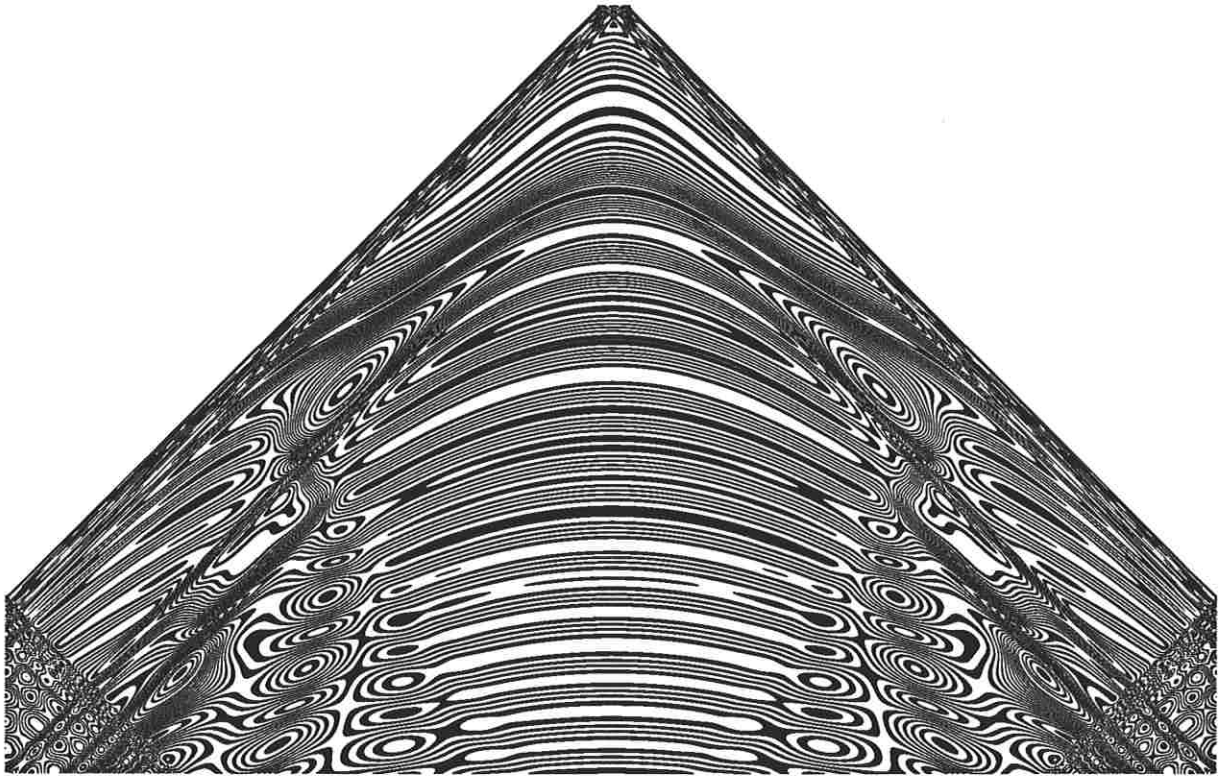

Figure 10C

Contours of Solution to

$$u_{tt} = u_{xx} + u(1-u^2)(1+4u)$$

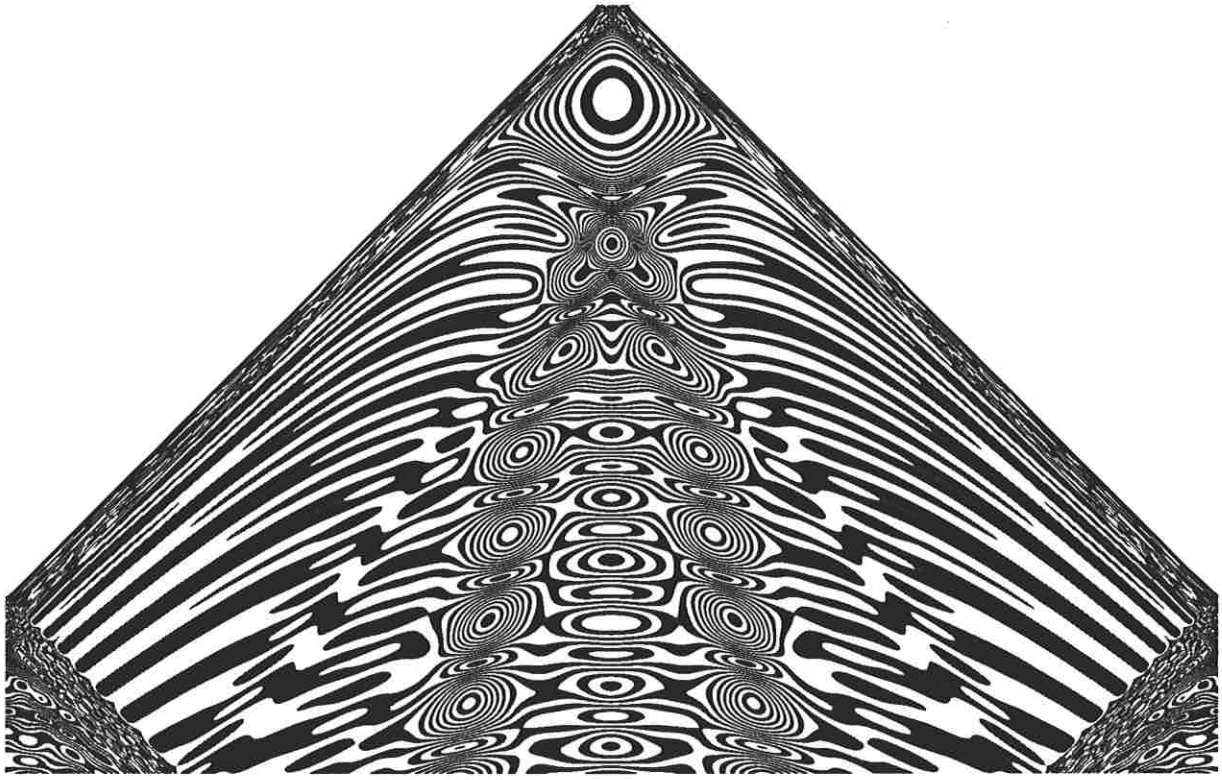

Figure 10D

Contours of Solution to

$$u_{tt} = u_{xx} + 2u^2(1-u^2)(1+4u)$$

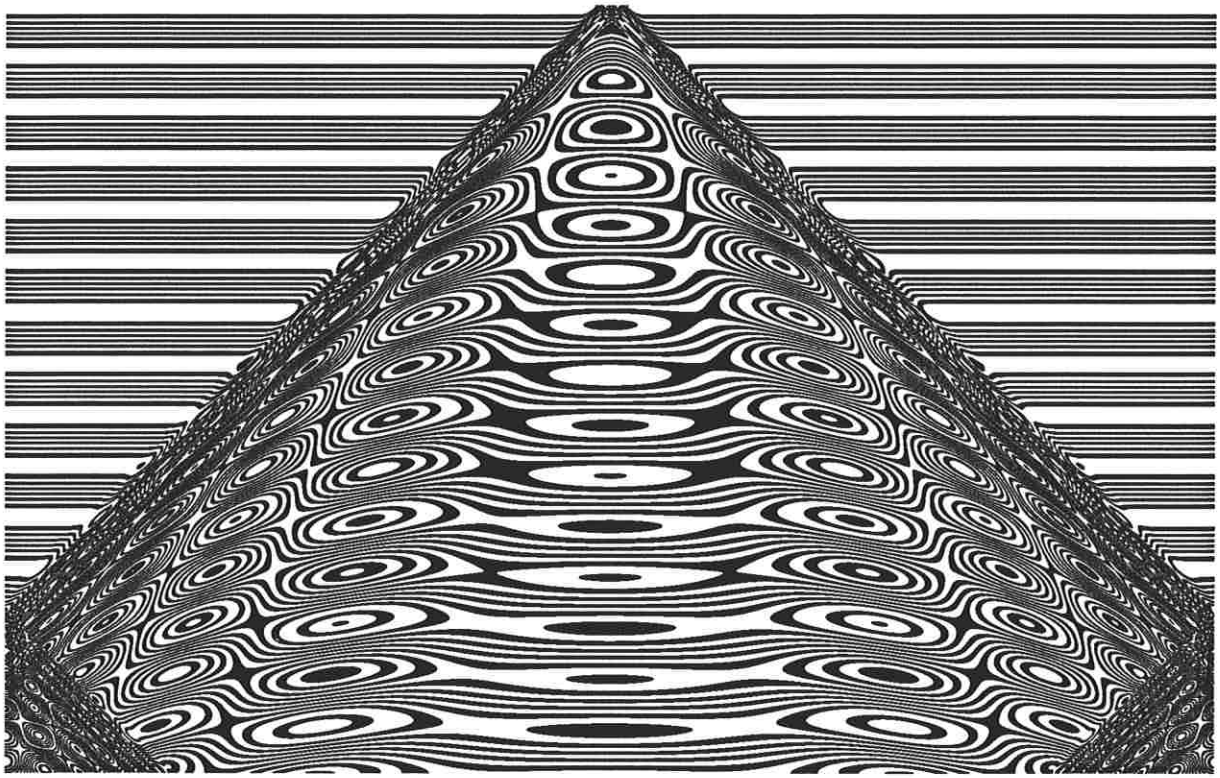

Figure 11A

Contours of Solution to

$$u_{tt} = u_{xx} + 1 - 4\sin u$$

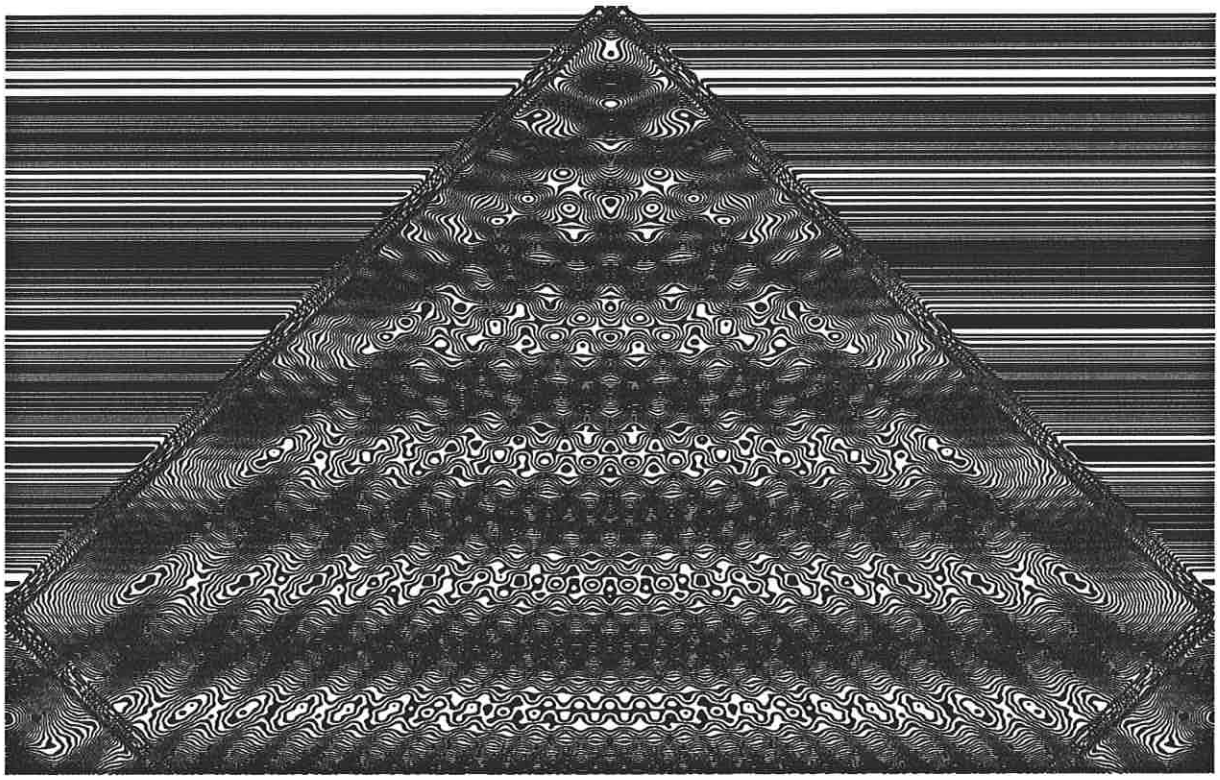

Figure 11B

Contours of Solution to

$$u_{tt} = u_{xx} + 1 + 4 \sin u$$

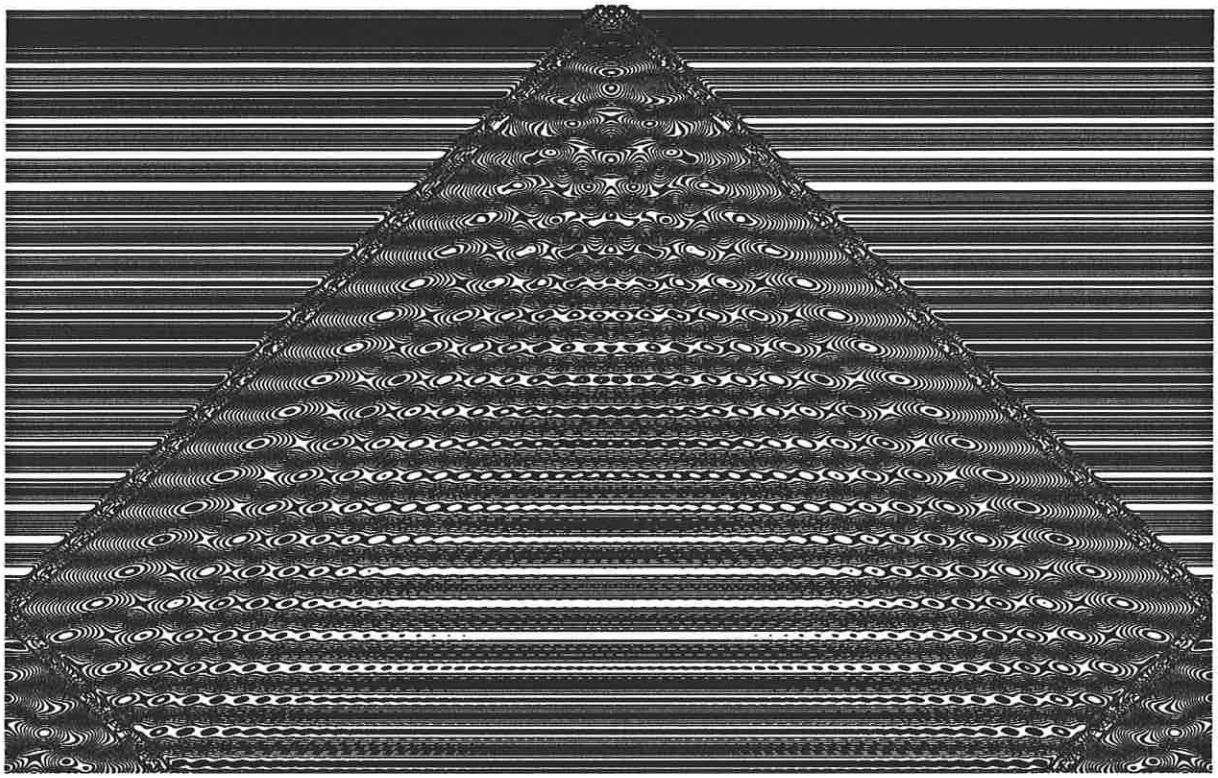

Figure 11C

Contours of Solution to

$$u_{tt} = u_{xx} + 4(1 - \sin u)$$

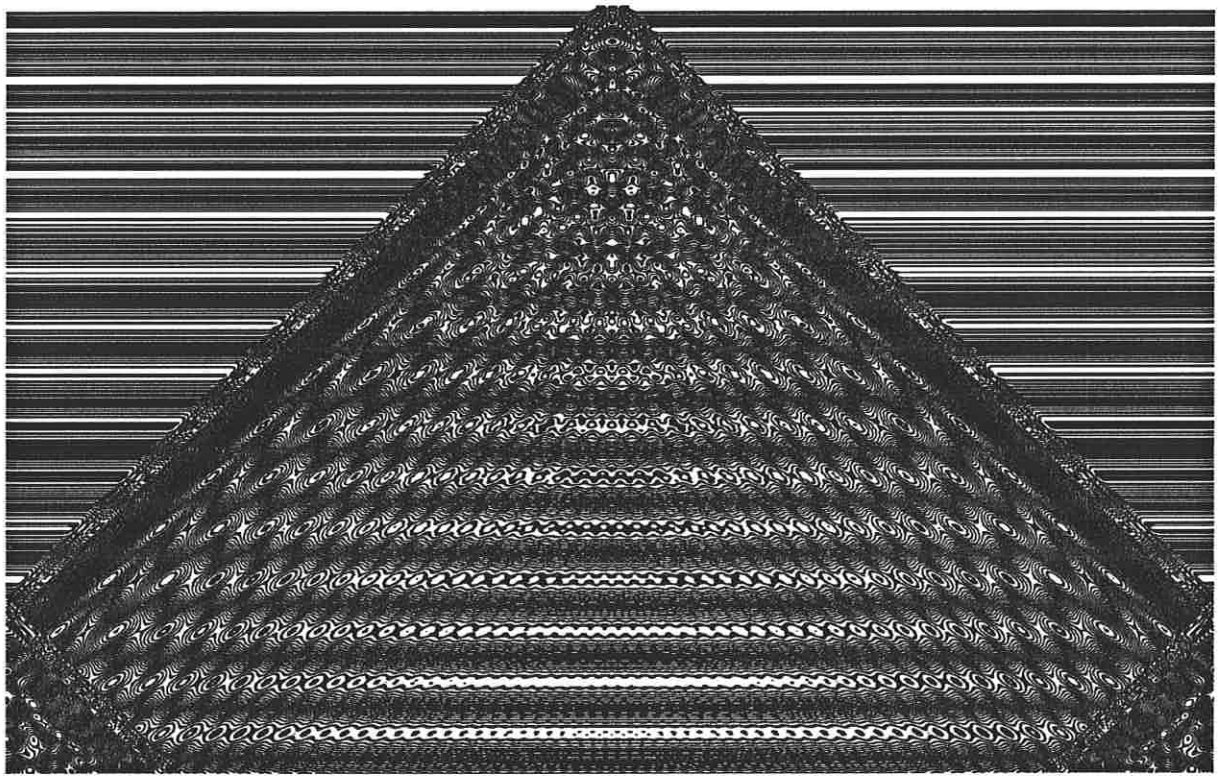

Figure 11D

Contours of Solution to

$$u_{tt} = u_{xx} + \frac{5}{2}(1 + 4\sin u)$$

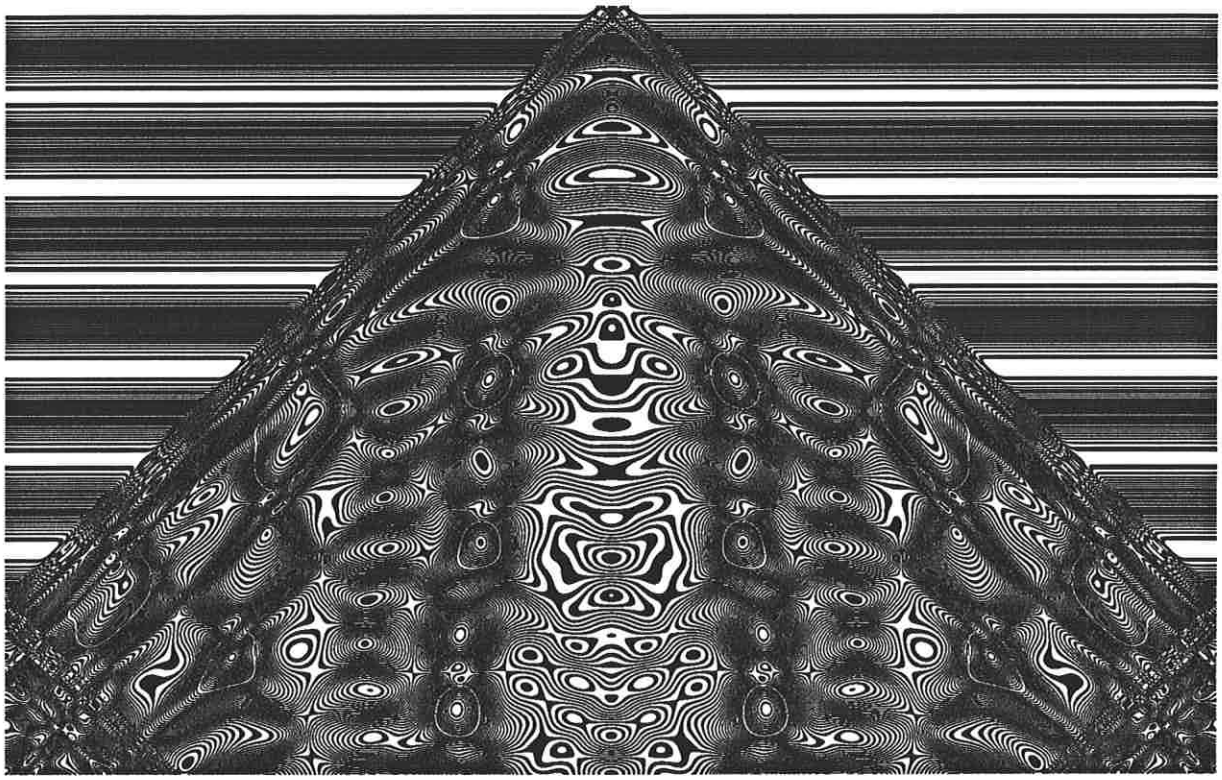

Figure 12A

Contours of Solution to

$$u_{tt} = u_{xx} + (1 + 4\sin u)\cos u$$

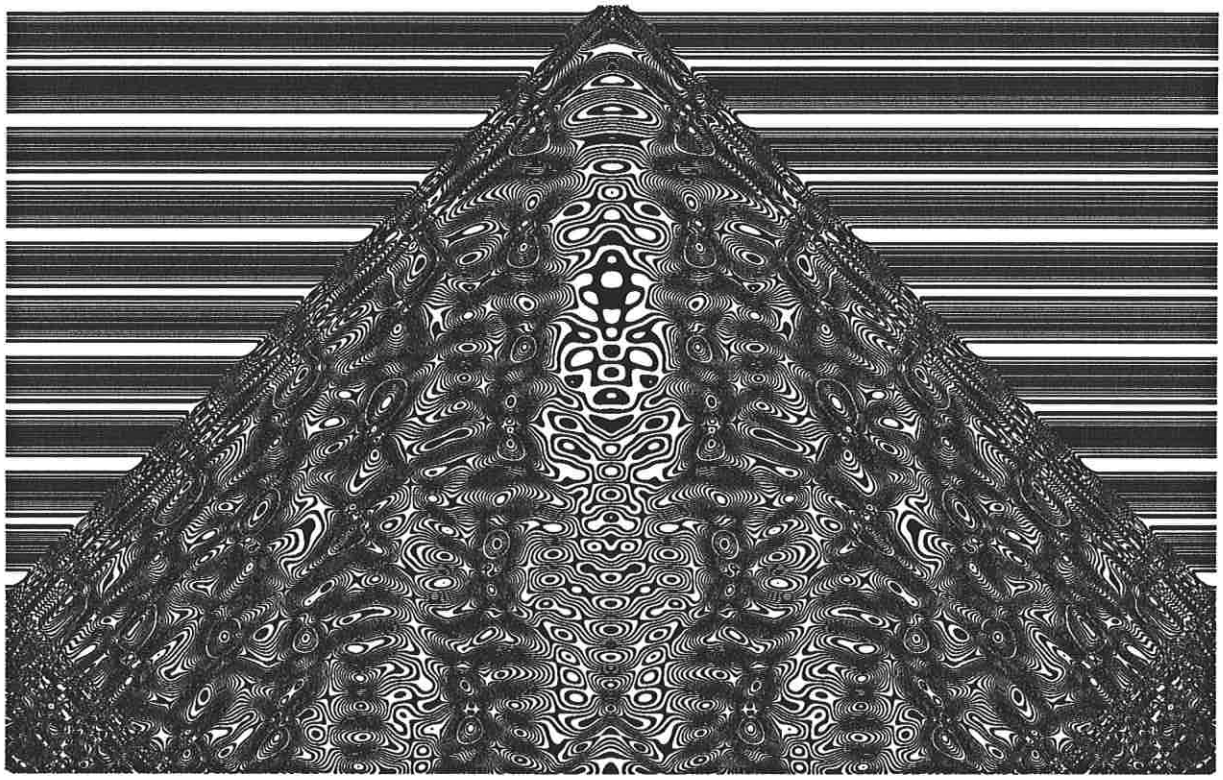

Figure 12B

Contours of Solution to

$$u_{tt} = u_{xx} + \frac{5}{2}(1 + 4\sin u)\cos u$$

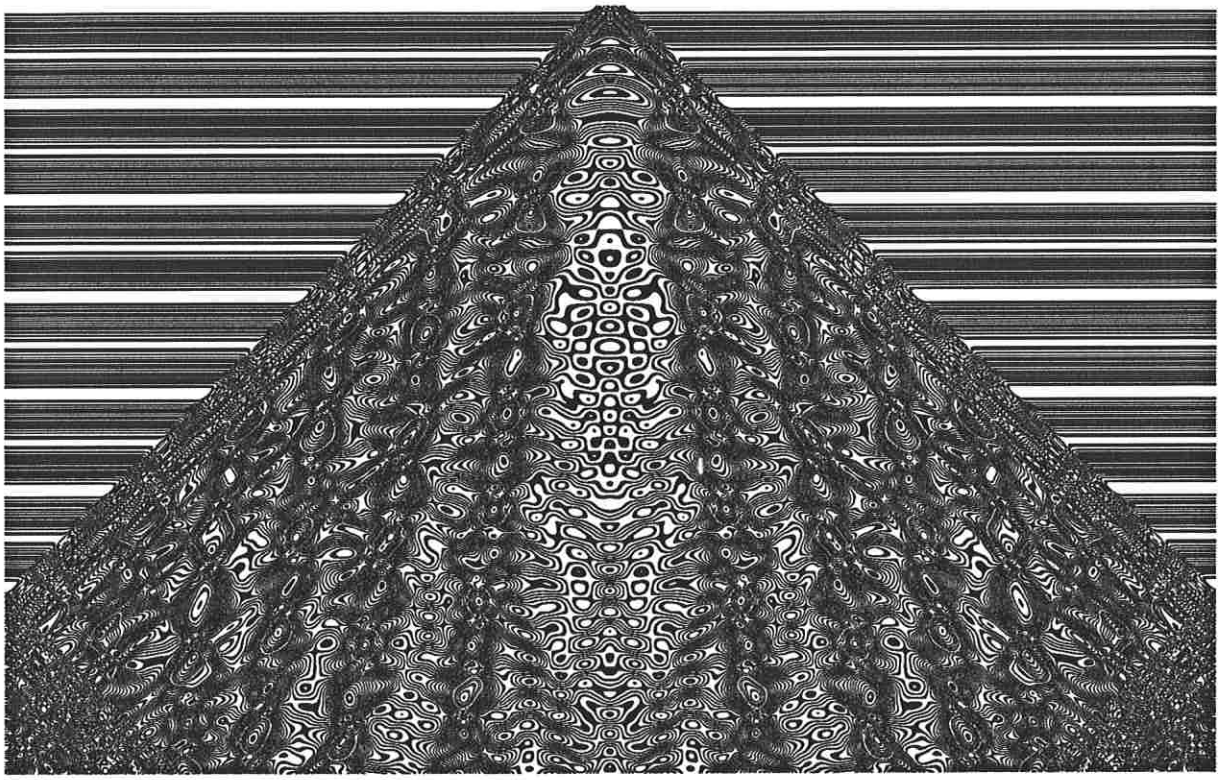

Figure 12C

Contours of Solution to

$$u_{tt} = u_{xx} + \frac{7}{2}(1 + 4\sin u)\cos u$$

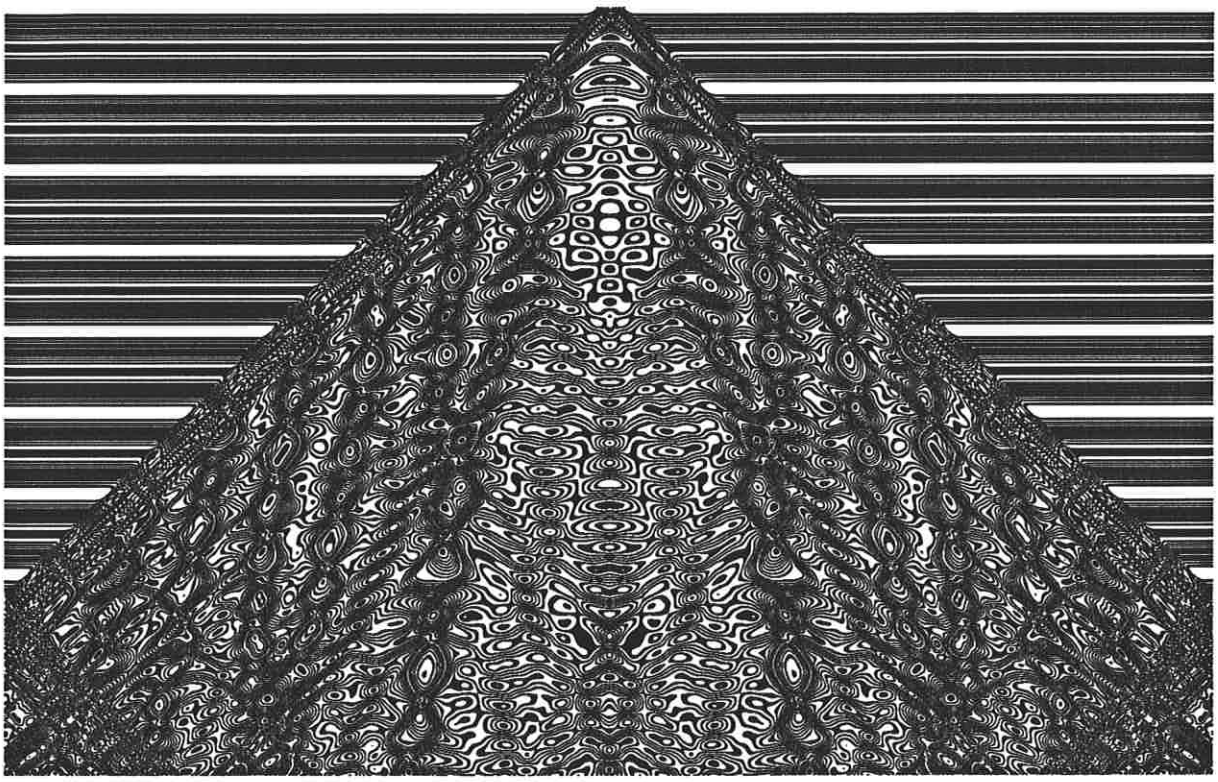

Figure 12D

Contours of Solution to

$$u_{tt} = u_{xx} + 5(1 + 4\sin u)\cos u$$

References

[T] M. Taylor, Difference Schemes for ODE, Lecture Notes, 1990.

[W] S. Wolfram, A New Kind of Science, Wolfram Media, 2002.